IEEE Access
Multidisciplinary ⋮ Rapid Review ⋮ Open Access Journal

Received June 8, 2021, accepted June 22, 2021, date of publication June 28, 2021, date of current version July 12, 2021.

Digital Object Identifier 10.1109/ACCESS.2021.3092830

Exploiting Secrecy Performance of Uplink NOMA in Cellular Networks

MINH-SANG VAN NGUYEN[1], DINH-THUAN DO[2] (Senior Member, IEEE), FATEMEH AFGHAH[3] (Senior Member, IEEE), S. M. RIAZUL ISLAM[4] (Member, IEEE), AND ANH-TU LE[5]

[1]Faculty of Electronics Technology, Industrial University of Ho Chi Minh City (IUH), Ho Chi Minh City 700000, Vietnam
[2]Department of Computer Science and Information Engineering, College of Information and Electrical Engineering, Asia University, Taichung 41354, Taiwan
[3]School of Informatics, Computing, and Cyber Systems, Northern Arizona University, Flagstaff, AZ 86011, USA
[4]Department of Computer Science and Engineering, Sejong University, Seoul 05006, South Korea
[5]Faculty of Information Technology, Van Lang University, Ho Chi Minh City 700000, Vietnam

Corresponding author: Anh-Tu Le (tule.iuh@gmail.com)

This work was supported in part by the Air Force Office of Scientific Research under Award FA9550-20-1-0090, and in part by the National Science Foundation under Grant CNS-2034218.

ABSTRACT We study the secrecy transmission of uplink non-orthogonal multiple access (NOMA) with single antenna and multi-antenna users in presence of an eavesdropper. Two phases are required for communications during each time frame between the users and the base station in cellular networks. We study the case where an eavesdropper overhears the relay and direct links from the users to the base stations. In terms of the secure performance analysis, we focus on two main metrics including secrecy outage probability (SOP) and strictly positive secrecy capacity (SPSC) with the assumption that the eavesdropper is able to detect the signals. Analytical closed-form expressions for the SOP and SPSC are derived to evaluate the system secure performance achieved by the proposed schemes. Furthermore, the asymptotic analysis is presented to gain further insights. The analytical and numerical results indicate that the proposed schemes can realize better secrecy performance once we improve the channel condition and signal-to-noise ratio (SNR) at the base station. Our results confirms that the secrecy performance gaps exist among the two users since different power allocation factors are assigned to these users.

INDEX TERMS Physical layer security, non-orthogonal multiple access, secrecy outage probability, strictly positive secrecy capacity.

I. INTRODUCTION

Due to superior spectral efficiency offeblack by NOMA, such promising multiple access technique is proposed for 5G networks [1]–[5]. Enabling superimposing multiple users in the power domain at the transmitter and requiring successive interference cancellation (SIC) at the receiver, differentiate NOMA from conventional orthogonal multiple access (OMA) technique was reported [6]. The multiple users can be served at the same time and frequency in the context of NOMA [7]. Based on the channel condition in NOMA system, the users are divided into different kinds of kinds such as the far users and the near users. However, the reliability of the far user depends on the existence of the near user [8]. In particular, to ensure user fairness the far user with poor channel condition is assigned with a higher power level compablack with the near user which has a good channel condition. It is beneficial in term of spectrum efficiency by employing multiple-input-multiple-output (MIMO) technologies in cooperative NOMA, as well as the interplay between cognitive radio and NOMA [8]. Especially, to achieve a balance between the performance of two users, cooperative NOMA techniques have been widely studied in recent work [9]–[16] along with various scenarios and system performance analysis. In cooperative NOMA schemes, the users located close to the base station (BS) can act as a relay to assist the far users. Particularly, the work in [10] explored a cooperative device-to-device (D2D) system with NOMA to allow the BS to simultaneously communicate with all users to satisfy the full information transmission

The associate editor coordinating the review of this manuscript and approving it for publication was Fakhrul Alam.

This work is licensed under a Creative Commons Attribution 4.0 License. For more information, see https://creativecommons.org/licenses/by/4.0/

requirement. They derived expressions in terms of the ergodic sum-rate (SR), outage probability and ergodic capacity. Meanwhile, the study in [12] indicated the remarkable outage performance gains of the scheme that combines the relay with the cooperative NOMA. The benefits of relay-assisted NOMA system can be reported if it is compared with the existing OMA schemes. In addition, the authors in [13] considered two modes of full-duplex (FD) and half-duplex (HD) to allow multiple relay nodes and a cell-center D2D device to support the transmission of a cell-edge D2D device. The authors calculated the closed-form expressions of the outage probabilities for both D2D users in different scenarios where the BS sends the signals to the far D2D user either through a near D2D user or multiple decode-and-forward (DF) relay nodes. In research of [14], the performance of a secondary network is determined in the system model which is enabled by a cognitive radio network with a NOMA scheme (namely CR-NOMA system) to serve many destination users. In particular, a D2D approach is implemented in the secondary network to further provide the signal transmission at a close distance of NOMA users in downlink. The performance of the NOMA users is studied under the interference received from the primary network.

The 5G and beyond wireless networks improve the performance of cellular users in term of security by introducing physical layer security (PLS) approaches [17]. Wyner in [18] first proposed PLS without exchanging secret keys where channel coding is regarded as the protection of information against eavesdropping signals. The PLS can benefit low-power devices (e.g. sensor networks) where traditional security methods do not work effectively. In fact, to enhance the overall system security, PLS techniques have been deployed in a wide range of RF applications to complement existing cryptography-based security approaches [19]. By leveraging features of the surrounding environments via sophisticated encoding schemes at the physical layer, the potential of PLS can be seen in recent work [20]. In [21], the authors explored secure downlink transmission in orthogonal frequency division multiplexing (OFDM)-assisted cognitive radio networks by allocating the power of the primary base station and cognitive base station (CBS) across different OFDM subcarriers in the presence of a multi-antenna eavesdropper. In [22], the authors studied a practical energy harvesting (EH) model by applying the secure transmit design for a downlink cognitive radio network using multiple-input-single-output (MISO). The authors in [23] considered a secure dual-hop mixed radio frequency-free space optical (RF-FSO) downlink by conducting energy harvesting protocol. The authors examined the secrecy outage probability (SOP) in the scenario such that the FSO link and all RF links follow Gamma-Gamma, independent, and identical Nakagami-*m* fading. In [24], the authors focused on heterogeneous networks and point-to-point systems to exhibit a comprehensive review on various multiple-antenna techniques in PLS together with transmit beamforming designs for multiple antenna nodes.

A. RELATED WORK

In [25], the authors presented exact analytic expressions to indicate secure performance such as SOP, average secrecy capacity (ASC), and probability of SPSC along with their insightful asymptotic computations. In addition, a particular case of mixed fading channels (Nakagami-*m*/Nakagami-*m*) is studied corresponding to formulas of ASC, SOP and SPSC. In [26], a hybrid free-space optical/radio frequency (FSO/RF) communication system is examined in terms of the secrecy performance. Since the eavesdropper tries to overhear the RF link between the legitimate transmitter and receiver of the hybrid system, secure performance need be analysed. Reference [27] introduced the secrecy measurements by deriving closed-form mathematical formulas of secure metrics such as SOP, ASC and SPSC. Reference [28] derived the exact SOP and the probability of SPSC expressions for two transmit antenna selection (TAS) mechanisms.

Despite various advantages of NOMA, it should be strengthen secure information for users accessing to the BS. Due to the broadcast characteristics of radio communications, NOMA users make the confidential information vulnerable to eavesdropping users. To this end, security provisioning of NOMA-aided systems is of critical importance, that calls for the application of PLS techniques to NOMA transmission. Considering PLS in NOMA systems [29-33], the authors in [29] studied the impact of PLS on the performance of a unified non-orthogonal multiple access (NOMA) framework by evaluating both external and internal eavesdroppers. The stochastic geometry approach is deployed for spatial distributions of eavesdroppers and legitimate users. The authors in [4] considered the multiple-antenna system for further enhancing the security of a beamforming-aided system where artificial noise is generated at the base station. The authors proved new exact formulas of the security outage probability for both single-antenna and multiple-antenna cases to evaluate the secrecy performance. The work in [30] focused on the PLS for massive MIMO systems with internal eavesdroppers. A new concept called secrecy area has been defined when near user was eavesdropped by the far user. The authors in [31] examined the sum achievable secrecy rate in a cellular downlink MISO-NOMA system. They considered a secure beamforming and power allocation design to achieve to maximal secure performance metric. The authors in [33] proposed reliable and secure communications with two optimal relay section schemes. In particular, they derived exact formulas of SOP and SPSC.

However, there are still only few works considering uplink NOMA system, in which the BS is under security threats when it processes the signals from massive users. In addition, the work on uplink cooperative NOMA in the aforementioned studies usually assume that there are direct links between the BS and the uplink users. In practice, the uplink users cannot transmit signals directly to the BS for some typical circumstances of small cells networks. To the best of the authors' knowledge, there are not much studies regarding the

uplink secure NOMA systems without direct links between the BS and the users, which motivates us to conduct this paper. However, in the scope of our study, we only consider particular circumstance in practice.

B. OUR CONTRIBUTIONS

NOMA is applicable in both uplink and downlink transmission systems since benefits of NOMA scheme are well proved. As discussed in aforementioned studies, most of the secure performance of NOMA networks are comprehensively analysed to raise performance gap among destinations. However, spectrum efficiency improvement in uplink is also crucial for 5G networks, which inspired this research. Further, motivated by the above observations [4], [29]–[33], we study in this paper a framework of a group of two NOMA users with respect to examine the security perspective of uplink NOMA transmissions in the presence of an eavesdropper. We further compare with similar studies to highlight our important contributions, shown in Table 1. In particular, the major contributions of this paper can be summarized as follows.

- This is one of few work considering the secure performance of uplink NOMA system with single antenna and multiple antennas at users when the direct and relay links from the user to the base station are enabled. In this regard, an eavesdropper is able to overhear information from both NOMA users.
- Corresponding to signal processing procedures at these phases, we compute the signal to interference plus noise ratio (SINR) to further achieve secure performance metrics, i.e. SOP and SPSC. The expressions of SOP and SPSC are derived in the closed-form. It can be found that the power allocation factors and the transmit SNR at the base station are main controlling coefficients that impact the secure performance as expected. We also consider a practical situation in which the relay cannot deploy SIC perfectly, the counterparts including the similar uplink NOMA with jammer selection and OMA schemes. To provide more insights, we obtain the approximate expressions of SOP to exhibit lower bounds of SOP for two users.
- By exploiting numerical simulations, our secure uplink NOMA schemes can guarantee the perfect security by adjusting the power allocation factors and limiting the impact of eavesdropper's signal, thus making our schemes very attractive for secure uplink NOMA transmissions in the deployment of NOMA in practice.

The remaining parts of this paper are organized as follows. Section II introduces the framework of secure cooperative uplink NOMA scenario by exploiting a single antenna two-user model. Section III and Section IV present the corresponding closed-form expressions and analyze the secrecy performance of SOP and SPSC respectively. Section V presents multi-antenna user case along performance analysis. Section VI provides numerical simulations and discussions. The paper is finally concluded in Section VII.

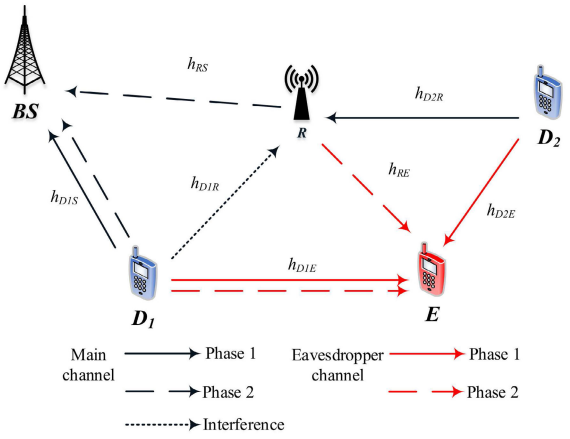

FIGURE 1. System model of secure uplink NOMA.

II. SECURE UPLINK NOMA WITH SINGLE ANTENNA: SYSTEM MODEL

The system model for the NOMA system is depicted in Fig. 1. This system contains the base station (BS), two users D_1 and D_2 employing the principle of NOMA in the uplink. Since D_2 is located at far cell-edge area, it needs assistance of a relay (R) to communicate with the BS (denoted as BS), user D_1 sends its signal directly to the BS. In the security perspective, an eavesdropper is able to overhear signals from nearby users including D_1, D_2 and relay R. Two phases of signal processing are adopted. The relay is required to decode the signal before communicating toward the base station. The system further requires a synchronous procedure to enable the two users to send their signals to the base station simultaneously. The wireless channels in such NOMA are subjected to Rayleigh flat fading plus additive white Gaussian noise. It is noted that the main parameters are shown in Table 2.

A. PHASE 1

Considering uplink NOMA [40], [41], the destinations D_1 and D_2 are able to communicate in the same time to the BS. The corresponding signals for two users are x_1 and x_2 which are allocated power portion as $\alpha_1 P$ and $\alpha_2 P$, respectively. It is noted simple allocation scheme is adopted due to simplicity in implementation of NOMA in practice, i.e. $\alpha_i P$, $(i = 1, 2)$ are the power allocation coefficients satisfying $\alpha_1 + \alpha_2 = 1$.[1] In the uplink manner, the transmit power levels at users are either a controlled transmit power or maximum power [40]. For many practical circumstance, the total transmit power requirement is crucial obeyed [41].

[1]Normally, the fixed power allocation approach is adopted to analyse the secure performance of various models regarding NOMA. Therefore, for implementation of an uplink secure NOMA transmission and to reduce overhead, such power allocation as well as channel state information (CSI) are still meaningful to study a performance analysis as presented in this study. The dynamic power allocation scheme is beyond the scope of this paper.

TABLE 1. Comparison of the proposed scheme with similar ideas.

	Our Scheme	[28]	[35]	[36]	[37]	[38]	[39]	[48]
NOMA	x		x	x	x	x	x	x
Uplink NOMA	x		x	x	x	x	x	
The security of uplink NOMA	x		x	x	x	x		
The uplink with assistance of a relay	x		x			x		
Imperfect SIC	x					x	x	
Interference from user to relay	x		x					
Multiple antennas at user	x							
Multiple users for uplink				x	x	x	x	
SOP	x	x		x				x
Asymptotic of SOP	x			x				x
SPSC	x	x						

TABLE 2. Main notations.

Symbol	Description
$\Pr(.)$	Probability
$F_Z(.)$	The cumulative distribution function (CDF) of a random variable Z
$f_Z(.)$	The probability density function (PDF) of a random variable Z
$\mathrm{Ei}\{.\}$	The exponential integral function
P	The total transmit power
ω_i, $(i = 1,2,3)$	The level of residual interference due to imperfect SIC at R from D_1, at BS from D_1 and at BS from R with $(0 \le \omega_i \le 1)$, such that $\omega = \omega_1 = \omega_2 = \omega_3$
R_{Di}	The target data rate for user D_i
σ_S	Additive white Gaussian noise (AWGN) noise variance at BS with $\sigma_S \sim CN(0, \vartheta^2)$
σ_R	AWGN noise variance at R with $\sigma_R \sim CN(0, \vartheta^2)$
σ_E	AWGN noise variance at E with $\sigma_E \sim CN(0, \vartheta_E^2)$
ϕ	The transmit SNR with $\phi = \frac{P}{\vartheta^2}$
h_{D1S}	The complex channel coefficient for the link $D_1 \to$ BS with $\lvert h_{D1S}\rvert^2 \sim CN(0, \lambda_{1S})$
h_{D1R}	The complex channel coefficient for the link $D_1 \to R$ with $h_{D1R} \sim CN(0, \lambda_{1R})$
h_{D2R}	The complex channel coefficient for the link $D_2 \to R$ with $h_{D2R} \sim CN(0, \lambda_{2R})$
h_{RS}	The complex channel coefficient for the link $R \to$ BS with $h_{RS} \sim CN(0, \lambda_{RS})$
h_{D1E}	The complex channel coefficient for the link $D_1 \to E$ with $h_{D1E} \sim CN(0, \lambda_{1E})$
h_{D2E}	The complex channel coefficient for the link $D_2 \to E$ with $h_{D2E} \sim CN(0, \lambda_{2E})$
h_{RE}	The complex channel coefficient for the link $R \to E$ with $h_{RE} \sim CN(0, \lambda_{RE})$

In this model, the received signal at the BS from D_1 in the first phase is given by [42]

$$y_{D1-S}^{(p1)} = h_{D1S}\sqrt{\alpha_1 P}x_1 + \sigma_S. \tag{1}$$

The signal to interference plus noise ratio (SINR) at the BS to receive signal from user D_1 is given by [42]

$$\gamma_{D1-S}^{(p1)} = \alpha_1\phi|h_{D1S}|^2. \tag{2}$$

On the other hand, the relay is able to receive signals from both two users D_i simultaneously under the assumption of perfect time synchronization between D_1 and D_2.

The relay can proceed signals in the first phase as [42]

$$y_R^{(p1)} = h_{D2R}\sqrt{\alpha_2 P}x_2 + h_{D1R}\sqrt{\alpha_1 P}x_1 + \sigma_R. \tag{3}$$

There are two possibilities to the relay can decode the symbol x_2 of D_2, i.e. namely G_1 and G_2 cases. It is worth noting that in the uplink NOMA, the decoding order gives higher priority for the user having better channel condition compared to the user having worse channel condition.

Case 1 (G_1): depending how strong two channels are. For the case G_1, condition on $h_{D1R} > h_{D2R}$, by treating the other user symbol (i.e. x_2) subject to the inferior link quality as noise, the relay R first decodes the user symbol (x_1) subject to the better link quality [42]. It is noted that G_i-D_i refers to user D_i with condition G_i. In this context, we can calculate the SINR of R as

$$\gamma_{R,1}^{(p1)} = \frac{\alpha_2\phi|h_{D2R}|^2}{\alpha_1\phi\left|\widetilde{h}_{D1R}\right|^2 + 1}, \tag{4}$$

where $\widetilde{h}_{D1R} \sim CN(0, \omega_1\lambda_{ip1})$. As a special case, $\omega_1 = 0$ denotes perfect SIC, whereas $\omega_1 = 1$ means that no SIC is performed at R.

Case 2: By contrast, $h_{D1R} < h_{D2R}$ corresponds to the condition G_2. In this circumstance, R has higher priority to decode signal x_2 for the better link quality and signal x_1 is treated as the inferior link or noise [42]. In particular, we examine the SINR at the relay R as

$$\gamma_{R,2}^{(p1)} = \frac{\alpha_2\phi|h_{D2R}|^2}{\alpha_1\phi|h_{D1R}|^2 + 1}. \tag{5}$$

The received signal at E from D_i $(i = 1, 2)$ in the first phase is given by[2]

$$y_E^{(p1)} = h_{D1E}\sqrt{\alpha_1 P}x_1 + h_{D2E}\sqrt{\alpha_2 P}x_2 + \sigma_E. \tag{6}$$

In this study, we suppose that the eavesdropper has a multi-user detection capability. In particular, a parallel interference cancellation (PIC) technique is employed at the eavesdropper to decode the superposed signal of D_i. Hence, the received SINR at eavesdropper to detect D_i's message can be written as [43]

$$\gamma_{Di-E}^{(p1)} = \alpha_i\phi_E|h_{DiE}|^2, \tag{7}$$

where $\phi_E = \frac{P}{\vartheta_E^2}$.

[2]We consider the secure scenario of the uplink NOMA in practical situation, such that a group of two users along with the existence an eavesdropper, in which the eavesdroppers are assumed to have enough detection capabilities to distinguish data stream processed in the same group [4], [5]. It is also assumed that the received signal from other group is too small that the data stream cannot be distinguished.

B. PHASE 2

In second phase, as main role of the relay R, it re-transmits the decoded symbol x_2 with power $\beta_2 P$ while D_1 processes ti transmit a new data symbol y_1 with power $\beta_1 P$ simultaneously. Note that $\beta_1 + \beta_2 = 1$, where β_i are the power allocation factors. The received signal at BS in the second phase is given by

$$y_S^{(p2)} = h_{D1S}\sqrt{\beta_1 P}y_1 + h_{RS}\sqrt{\beta_2 P}x_2 + \sigma_S. \quad (8)$$

Case 1: In the case when $h_{D1R} > h_{RS}$, the BS treats signal x_2 as noise to first decode y_1. It is noted that SIC is required to decode y_1. We compute SINRs at the BS to decode signals y_1, x_2 respectively by [42]

$$\gamma_{y_1}^{(p2)} = \frac{\beta_1\phi|h_{D1S}|^2}{\beta_2\phi|h_{RS}|^2 + 1}, \quad (9)$$

$$\gamma_{x_2}^{(p2)} = \frac{\beta_2\phi|h_{RS}|^2}{\beta_1\phi\left|\widetilde{h}_{D1S}\right|^2 + 1}, \quad (10)$$

where $\widetilde{h}_{D1S} \sim CN\left(0, \omega_2\lambda_{ip2}\right)$.

Case 2: By considering the case such that $h_{D1R} < h_{RS}$, the BS treats y_1 as noise to decode x_2. Similarly, we can obtain SINRs at the BS corresponding to decode x_2, y_1 respectively as

$$\gamma_{x_{2,2}}^{(p2)} = \frac{\beta_2\phi|h_{RS}|^2}{\beta_1\phi|h_{D1S}|^2 + 1}, \quad (11)$$

$$\gamma_{y_{1,2}}^{(p2)} = \frac{\beta_1\phi|h_{D1S}|^2}{\beta_2\phi\left|\widetilde{h}_{RS}\right|^2 + 1}, \quad (12)$$

where $\widetilde{h}_{RS} \sim CN\left(0, \omega_3\lambda_{ip3}\right)$. The solution for the second case is similar as the first case. We do not consider details for the second case here.

The received signal at E from R and D_1 can give by

$$y_E^{(p2)} = h_{D1E}\sqrt{\beta_1 P}y_1 + h_{RE}\sqrt{\beta_2 P}x_2 + \sigma_E. \quad (13)$$

After PIC, the received SINR at the eavesdropper to detect D_i's message can be written as

$$\gamma_{Di-E}^{(p2)} = \beta_i\phi_E|h_X|^2, \quad (14)$$

where $X = \{D1E, RE\}$.

The sum achievable secrecy rates of D_1 is written as [42]–[44]

$$\begin{aligned} C_{D1} &= \left[\frac{1}{2}\log_2\left(\frac{1+\gamma_{D1-S}^{(p1)}}{1+\gamma_{D1-E}^{(p1)}}\right)\right]^+ \\ &\quad + \left[\frac{1}{2}\log_2\left(\frac{1+\gamma_{y_1}^{(p2)}}{1+\gamma_{D1-E}^{(p2)}}\right)\right]^+ \\ &= C_{D1}^{(p1)} + C_{D1}^{(p2)}, \end{aligned} \quad (15)$$

where $[x]^+ = \max\{0, x\}$.

Based on obtained SINRs, we can determine the achievable secrecy rates corresponding two conditions $G1$, $G2$ which can be further examined by using results in (4), (5), (7) and (10) as

$$C_{D2}^{(G1)} = \frac{1}{2}\left[\log_2\min\left(\frac{1+\gamma_{R,1}^{(p1)}}{1+\gamma_{D2-E}^{(p1)}}, \frac{1+\gamma_{x_2}^{(p2)}}{1+\gamma_{D2-E}^{(p2)}}\right)\right]^+, \quad (16)$$

$$C_{D2}^{(G2)} = \frac{1}{2}\left[\log_2\min\left(\frac{1+\gamma_{R,2}^{(p1)}}{1+\gamma_{D2-E}^{(p1)}}, \frac{1+\gamma_{x_2}^{(p2)}}{1+\gamma_{D2-E}^{(p2)}}\right)\right]^+. \quad (17)$$

III. ANALYSIS OF SOP

To evaluate the security performance of the considered uplink system, we expect to compute expressions of SOP. However, before achieving SOP we need distributions of related channels. SOP is can be defined as the probability that the secrecy capacity is less than a given target rate.

It is noted that all channels follow the Rayleigh distribution with CDF and PDF can be expressed respectively by [42]

$$F_{|U|^2}(x) = 1 - \exp\left(-\frac{x}{V}\right), \quad (18)$$

$$f_{|U|^2}(x) = \frac{1}{V}\exp\left(-\frac{x}{V}\right), \quad (19)$$

where $U \in \left\{h_{D1S}, \widetilde{h}_{D1S}, h_{D1R}, \widetilde{h}_{D1R}, h_{D2R}, h_{RS}, \widetilde{h}_{RS}, h_{D1E}, h_{D2E}, h_{RE}\right\}$ and $V \in \left\{\lambda_{1S}, \omega_2\lambda_{ip2}, \lambda_{1R}, \omega_1\lambda_{ip1}, \lambda_{2R}, \lambda_{RS}, \omega_3\lambda_{ip3}, \lambda_{1E}, \lambda_{2E}, \lambda_{RE}\right\}$.

A. SOP OF D_1

In uplink NOMA systems, we refer to the ability to decode D_1's signal at the BS. The secure outage can be determined by considering possibility such that $C_{D1}^{(p1)}$ or $C_{D1}^{(p2)}$ falls below their own target rates. In particular, the SOP at the BS for decoding D_1's signal is given by [43]

$$\begin{aligned} SOP_{D1} &= \Pr\left(C_{D1}^{(p1)} < R_{D1} \text{ or } C_{D1}^{(p2)} < R_{D1}\right) \\ &= 1 - \Pr\left[\frac{1+\gamma_{D1-S}^{(p1)}}{1+\gamma_{D1-E}^{(p1)}} \geq \mu_1, \frac{1+\gamma_{y_1}^{(p2)}}{1+\gamma_{D1-E}^{(p2)}} < \mu_1\right]. \end{aligned} \quad (20)$$

Proposition 1: The closed-form expression of SOP for D_1 can be expressed by

$$\begin{aligned} SOP_{D1} &= 1 + \frac{\phi\lambda_{1S}}{\mu_1\phi_E\lambda_{1E} + \phi\lambda_{1S}}\frac{\lambda_{1S}}{\mu_1\phi_E\beta_2\lambda_{1E}\lambda_{RS}} \\ &\quad \times \exp\left(\bar{\lambda}\theta - \frac{\overline{\mu_1}}{\beta_1\phi\lambda_{1S}} - \frac{\overline{\mu_1}}{\alpha_1\phi\lambda_{1S}}\right)\mathrm{Ei}\left(-\bar{\lambda}\theta\right), \end{aligned} \quad (21)$$

where $\theta = \frac{\mu_1\phi_E\lambda_{1E}+\phi\lambda_{1S}}{\mu_1\phi_E\phi\beta_2\lambda_{1E}}$, $\mu_i = 2^{2R_{Di}}$, $\overline{\mu_i} = \mu_i - 1$, $i \in \{1, 2\}$, $\bar{\lambda} = \frac{\overline{\mu_1}\beta_2}{\beta_1\lambda_{1S}} + \frac{1}{\lambda_{RS}}$.

Proof: See Appendix A.

B. SOP OF D_2

By treating two conditions $G1$ and $G2$, we need to compute the SOP of D_2's signal in the closed-form.

1) SOP OF D_2: CASE $G1$

From (16), the SOP of user D_2 can be expressed as

$$\begin{aligned} SOP_{D2}^{(G1)} &= \Pr\left[C_{D2}^{(G1)} < R_{D2}\right] \\ &= 1 - \Pr\left[\min\left(\frac{1+\gamma_{R,1}^{(p1)}}{1+\gamma_{D2-E}^{(p1)}}, \frac{1+\gamma_{x_2}^{(p2)}}{1+\gamma_{D2-E}^{(p2)}}\right) \geq \mu_2\right] \\ &= 1 - \underbrace{\Pr\left[\frac{1+\gamma_{R,1}^{(p1)}}{1+\gamma_{D2-E}^{(p1)}} \geq \mu_2\right]}_{B_1} \underbrace{\Pr\left[\frac{1+\gamma_{x_2}^{(p2)}}{1+\gamma_{D2-E}^{(p2)}} \geq \mu_2\right]}_{B_2}. \end{aligned} \quad (22)$$

Proposition 2: The closed-form expression of SOP for D_2 corresponding to case $G1$ can be expressed by

$$\begin{aligned} SOP_{D2}^{(G1)} = 1 &- \frac{\lambda_{2R}}{\mu_2\alpha_1\phi_E\omega_1\lambda_{ip1}\lambda_{2E}} \frac{\lambda_{RS}}{\mu_2\beta_1\phi_E\omega_2\lambda_{ip2}\lambda_{RE}} \\ &\times \exp\left(\psi_1\delta_1 - \frac{\overline{\mu_2}}{\alpha_2\phi\lambda_{2R}} + \psi_2\delta_2 - \frac{\overline{\mu_2}}{\beta_2\phi\lambda_{RS}}\right) \\ &\times \mathrm{Ei}\left(-\psi_1\delta_1\right)\mathrm{Ei}\left(-\psi_2\delta_2\right), \end{aligned} \quad (23)$$

where $\psi_1 = \frac{\mu_2\phi_E\lambda_{2E}+\phi\lambda_{2R}}{\mu_2\alpha_1\phi\phi_E\lambda_{2E}}$, $\psi_2 = \frac{\mu_2\phi_E\lambda_{RE}+\phi\lambda_{RS}}{\mu_2\beta_1\phi_E\phi\lambda_{RE}}$, $\delta_1 = \frac{\overline{\mu_2}\alpha_1}{\alpha_2\lambda_{2R}} + \frac{1}{\omega_1\lambda_{ip1}}$, $\delta_2 = \frac{\overline{\mu_2}\beta_1}{\beta_2\lambda_{RS}} + \frac{1}{\omega_2\lambda_{ip2}}$.

Proof: See Appendix B.

2) SOP OF D_2: CASE $G2$

From (17), the SOP of D_2 can be expressed as

$$\begin{aligned} SOP_{D2}^{(G2)} &= \Pr\left[C_{D2}^{(G2)} < R_{D2}\right] \\ &= 1 - \Pr\left[\min\left(\frac{1+\gamma_{R,2}^{(p1)}}{1+\gamma_{D2-E}^{(p1)}}, \frac{1+\gamma_{x_2}^{(p2)}}{1+\gamma_{D2-E}^{(p2)}}\right) \geq \mu_2\right] \\ &= 1 - \underbrace{\Pr\left[\frac{1+\gamma_{R,2}^{(p1)}}{1+\gamma_{D2-E}^{(p1)}} \geq \mu_2\right]}_{C_1} \underbrace{\Pr\left[\frac{1+\gamma_{x_2}^{(p2)}}{1+\gamma_{D2-E}^{(p2)}} \geq \mu_2\right]}_{B_2}. \end{aligned} \quad (24)$$

Proposition 3: The closed-form expression of SOP for D_2 corresponding to case $G2$ can be formulated by

$$\begin{aligned} SOP_{D2}^{(G2)} = 1 &- \frac{\lambda_{2R}}{\mu_2\alpha_1\phi_E\lambda_{1R}\lambda_{2E}} \frac{\lambda_{RS}}{\mu_2\beta_1\phi_E\omega_2\lambda_{ip2}\lambda_{RE}} \\ &\times \exp\left(\psi_1\chi - \frac{\overline{\mu_2}}{\alpha_2\phi\lambda_{2R}} + \psi_2\delta_2 - \frac{\overline{\mu_2}}{\beta_2\phi\lambda_{RS}}\right) \\ &\times \mathrm{Ei}\left(-\psi_1\chi\right)\mathrm{Ei}\left(-\psi_2\delta_2\right), \end{aligned} \quad (25)$$

where $\chi = \frac{\overline{\mu_2}\alpha_1}{\alpha_2\lambda_{2R}} + \frac{1}{\lambda_{1R}}$.

Proof: From (24), C_1 can be calculated as (26), where the CDF of $|h_{D2R}|^2$, the PDF of $|h_{D2E}|^2$ and $|h_{D1R}|^2$ base on (18) and (19), shown at the bottom of the next page.

Based on [45, Eq. (3.352.4)] and applying some polynomial expansion manipulations, C_1 is written by

$$\begin{aligned} C_1 = -\frac{\lambda_{2R}}{\mu_2\alpha_1\phi_E\lambda_{1R}\lambda_{2E}} &\exp\left(-\frac{\overline{\mu_2}}{\alpha_2\phi\lambda_{2R}}\right) \\ &\times \exp\left(\psi_1\chi\right)\mathrm{Ei}\left(-\psi_1\chi\right). \end{aligned} \quad (27)$$

Substituting (27) into (24), (25) can be obtained.

The proof is completed.

To further analyse system performance, we can see that two conditions of successful decoding signal corresponding to the two phases lead to the variations of SOP performance. The target rates appear in expressions of SOP, for example (20), and therefore such target rates will limit improvement of secure performance. Although the ergodic secrecy rate is also important, but the SOP is at a higher priority to examine the secure performance of such kind of uplink NOMA.

Remark 1: Since expressions of SOP are so complicated, we examine the main factors affecting the SOP performance. For example, (25) contains the parameters ϕ, ϕ_E and the channel gains, and hence the secure performance metrics depend mainly on these parameters. As a result, it can be concluded which parameters can be improved to obtain the best security behavior. The reason for the imbalance in the performance of two users is the power allocation factors which appear in coefficient χ. Further, we should note that the SOP performance can be improved when ϕ increases.

C. ASYMPTOTIC OF SOP

When $\phi \to \infty$ and based on (A.1)-(A.3), the asymptotic SOP of D_1 is given by

$$\begin{aligned} SOP_{D1}^{asym} &= 1 - \frac{1}{\lambda_{RS}}\int_0^\infty \exp\left(-\left(\frac{\overline{\mu_1}\beta_2}{\beta_1\lambda_{1S}} + \frac{1}{\lambda_{RS}}\right)y\right)dy \\ &= 1 - \frac{\beta_1\lambda_{1S}}{\overline{\mu_1}\beta_2\lambda_{RS} + \beta_1\lambda_{1S}}. \end{aligned} \quad (28)$$

Similarly, from (28), (B.1) and (B.3), when $\phi \to \infty$ the asymptotic SOP of D_2 for the case $G1$ is given by

$$\begin{aligned} SOP_{D2}^{(G1,asym)} &= 1 - \frac{1}{\omega_1\lambda_{ip1}}\frac{1}{\omega_2\lambda_{ip2}} \\ &\times \int_0^\infty \exp\left(-\left(\frac{\overline{\mu_2}\alpha_1}{\alpha_2\lambda_{2R}} + \frac{1}{\omega_1\lambda_{ip1}}\right)x\right)dx \\ &\times \int_0^\infty \exp\left(-\left(\frac{\overline{\mu_2}\beta_1}{\beta_2\lambda_{RS}} + \frac{1}{\omega_2\lambda_{ip2}}\right)y\right)dy \\ &= 1 - \frac{\alpha_2\lambda_{2R}}{\overline{\mu_2}\alpha_1\omega_1\lambda_{ip1} + \alpha_2\lambda_{2R}}\frac{\beta_2\lambda_{RS}}{\overline{\mu_2}\beta_1\omega_2\lambda_{ip2} + \beta_2\lambda_{RS}}. \end{aligned} \quad (29)$$

Next, from (26) and (B.3), when $\phi \to \infty$, the asymptotic SOP of D_2 for the case $G2$ is computed by

$$\begin{aligned} SOP_{D2}^{(G2,asym)} &= 1 - \frac{1}{\lambda_{1R}}\frac{1}{\omega_2\lambda_{ip2}} \\ &\times \int_0^\infty \exp\left(-\left(\frac{\overline{\mu_2}\alpha_1}{\alpha_2\lambda_{2R}} + \frac{1}{\lambda_{1R}}\right)x\right)dx \\ &\times \int_0^\infty \exp\left(-\left(\frac{\overline{\mu_2}\beta_1}{\beta_2\lambda_{RS}} + \frac{1}{\omega_2\lambda_{ip2}}\right)y\right)dy \\ &= 1 - \frac{\alpha_2\lambda_{2R}}{\overline{\mu_2}\alpha_1\lambda_{1R} + \alpha_2\lambda_{2R}}\frac{\beta_2\lambda_{RS}}{\overline{\mu_2}\beta_1\omega_2\lambda_{ip2} + \beta_2\lambda_{RS}}. \end{aligned} \quad (30)$$

Remark 2: In order to gain more insights, such system's asymptotic behavior obtained in this section is necessary when the transmit SNR at destinations are sufficiently large. In particular, when $\phi \to \infty$, the expressions of asymptotic SOP in (28), (29), and (30) mainly depend on system parameters such as target rates, channel gains and power allocation factors. Therefore, we predict that such SOP is likely saturated lines at high region of ϕ.

IV. SPSC ANALYSIS

A. SPSC OF D_1

Another main performance metric is SPSC, which is the fundamental benchmark for secrecy performance and denotes the probability of existence of the secrecy capacity [43]. Thus, the SPSC of D_1 is readily given by

$$\begin{aligned} SPSC_{D1} &= \Pr\left(C_{D1}^{(p1)} > 0, C_{D1}^{(p2)} > 0\right) \\ &= \underbrace{\Pr\left(\gamma_{D1-S}^{(p1)} > \gamma_{D1-E}^{(p1)}\right)}_{Q_1} \underbrace{\Pr\left(\gamma_{y_1}^{(p2)} > \gamma_{D1-E}^{(p2)}\right)}_{Q_2}. \end{aligned} \quad (31)$$

Proposition 4: The closed-form expression of SPSC for D_1 can be expressed by

$$\begin{aligned} SPSC_{D1} = -\frac{\phi\lambda_{1S}}{\phi_E\lambda_{1E} + \phi\lambda_{1S}} \frac{\lambda_{1S}}{\beta_2\phi_E\lambda_{1E}\lambda_{RS}} \\ \times \exp\left(\Phi_1\right) \mathrm{Ei}\left(-\Phi_1\right), \end{aligned} \quad (32)$$

where $\Phi_1 = \frac{\phi_E\lambda_{1E}+\phi\lambda_{1S}}{\beta_2\phi_E\phi\lambda_{1E}\lambda_{RS}}$.

Proof: See Appendix C.

B. SPSC OF D_2

Case 1: The SPSC for $G_1 - D_2$ can be expressed as

$$\begin{aligned} SPSC_{D2}^{(G1)} &= \Pr\left[C_{D2}^{(G1)} > 0\right] \\ &= \underbrace{\Pr\left[\gamma_{R,1}^{(p1)} > \gamma_{D2-E}^{(p1)}\right]}_{W_1} \underbrace{\Pr\left[\gamma_{x_2}^{(p2)} > \gamma_{D2-E}^{(p2)}\right]}_{W_2}. \end{aligned} \quad (33)$$

Proposition 5: The closed-form expression of SPSC for $G_1 - D_2$ can be expressed by

$$\begin{aligned} SPSC_{D2}^{(G1)} = \frac{\lambda_{2R}}{\alpha_1\phi_E\lambda_{2E}\omega_1\lambda_{ip1}} \frac{\lambda_{RS}}{\beta_1\phi_E\lambda_{RE}\omega_2\lambda_{ip2}} \\ \times \exp\left(\Phi_2 + \Phi_3\right) \mathrm{Ei}\left(-\Phi_2\right) \mathrm{Ei}\left(-\Phi_3\right), \end{aligned} \quad (34)$$

where $\Phi_2 = \frac{\phi_E\lambda_{2E}+\phi\lambda_{2R}}{\alpha_1\phi\phi_E\lambda_{2E}\omega_1\lambda_{ip1}}$, $\Phi_3 = \frac{\phi_E\lambda_{RE}+\phi\lambda_{RS}}{\beta_1\phi\phi_E\lambda_{RE}\omega_2\lambda_{ip2}}$.

Proof: See Appendix D.

Case 2: Similar to $G_1 - D_2$, the SPSC for $G_2 - D_2$ case can be expressed as

$$\begin{aligned} SPSC_{D2}^{(G2)} &= \Pr\left[C_{D2}^{(G2)} > 0\right] \\ &= \underbrace{\Pr\left[\gamma_{R,2}^{(p1)} > \gamma_{D2-E}^{(p1)}\right]}_{\Theta_1} \underbrace{\Pr\left[\gamma_{x_2}^{(p2)} > \gamma_{D2-E}^{(p2)}\right]}_{W_2}. \end{aligned} \quad (35)$$

Proposition 6: The closed-form expression of SPSC for $G_2 - D_2$ can be expressed by

$$\begin{aligned} SPSC_{D2}^{(G2)} = \frac{\lambda_{2R}}{\alpha_1\phi_E\lambda_{2E}\lambda_{1R}} \frac{\lambda_{RS}}{\beta_1\phi_E\lambda_{RE}\omega_2\lambda_{ip2}} \\ \times \exp\left(\Phi_3 + \Phi_4\right) \mathrm{Ei}\left(-\Phi_3\right) \mathrm{Ei}\left(-\Phi_4\right), \end{aligned} \quad (36)$$

where $\Phi_4 = \frac{\phi_E\lambda_{2E}+\phi\lambda_{2R}}{\alpha_1\phi\phi_E\lambda_{2E}\lambda_{1R}}$.

Proof: From (35), Θ_1 can be calculated as (37), where the CDF of $|h_{D2R}|^2$, the PDF of $|h_{D2E}|^2$ and $|h_{D1R}|^2$ base on (18) and (19), shown at the bottom of the next page.

Substituting (37) into (35), (36) can be obtained and the proof is completed.

Remark 3: Similarly, since the same parameters lead to the enhancement of SOP, this section presents the expressions of SPSC performance which relate to the similar system parameters reported for SOP metric. For example, we examine the main factors affecting the SPSC performance in (36) which are ϕ, ϕ_E and the related channel gains, and hence secure performance metrics depend mainly on these parameters. As a result, by controlling these values, an improvement in the SOP and SPSC indicators can be achieved.

$$\begin{aligned} C_1 &= \Pr\left[\gamma_{R,2}^{(p1)} \geq \overline{\mu_2} + \mu_2\gamma_{D2-E}^{(p1)}\right] \\ &= \Pr\left[|h_{D2R}|^2 \geq \frac{\left(\overline{\mu_2} + \mu_2\alpha_2\phi_E|h_{D2E}|^2\right)\left(\alpha_1\phi|h_{D1R}|^2 + 1\right)}{\alpha_2\phi}\right] \\ &= \int_0^\infty \int_0^\infty \left(1 - F_{|h_{D2R}|^2}\left(\frac{\left(\overline{\mu_2} + \mu_2\alpha_2\phi_E x\right)\left(\alpha_1\phi y + 1\right)}{\alpha_2\phi}\right)\right) f_{|h_{D2E}|^2}(x) f_{|h_{D1R}|^2}(y)\, dxdy \\ &= \int_0^\infty \int_0^\infty \exp\left(-\frac{\left(\overline{\mu_2} + \mu_2\alpha_2\phi_E x\right)\left(\alpha_1\phi y + 1\right)}{\alpha_2\phi\lambda_{2R}}\right) \frac{1}{\lambda_{2E}} \exp\left(-\frac{x}{\lambda_{2E}}\right) \frac{1}{\lambda_{1R}} \exp\left(-\frac{y}{\lambda_{1R}}\right) dxdy \\ &= \frac{1}{\lambda_{2E}}\frac{1}{\lambda_{1R}} \exp\left(-\frac{\overline{\mu_2}}{\alpha_2\phi\lambda_{2R}}\right) \int_0^\infty \int_0^\infty \exp\left(-\left(\frac{\mu_2\alpha_1\phi_E\phi y + \mu_2\phi_E}{\phi\lambda_{2R}} + \frac{1}{\lambda_{2E}}\right)x\right) \exp\left(-\left(\frac{\overline{\mu_2}\alpha_1}{\alpha_2\lambda_{2R}} + \frac{1}{\lambda_{1R}}\right)y\right) dxdy \\ &= \frac{1}{\lambda_{1R}} \exp\left(-\frac{\overline{\mu_2}}{\alpha_2\phi\lambda_{2R}}\right) \int_0^\infty \frac{\phi\lambda_{2R}}{\mu_2\alpha_1\phi_E\phi\lambda_{2E}y + \mu_2\phi_E\lambda_{2E} + \phi\lambda_{2R}} \exp\left(-\left(\frac{\overline{\mu_2}\alpha_1}{\alpha_2\lambda_{2R}} + \frac{1}{\lambda_{1R}}\right)y\right) dy. \end{aligned} \quad (26)$$

V. EXTENSION TO MULTIPLE ANTENNAS AT USERS

In Fig. 2, two users may benefit by multi-antenna design. It is assumed that users D_1, D_2 are equipped with N and M antennas respectively [47]. For simplicity, the system treats its nodes in a half-duplex mode. The transmit antenna selection approach is adopted to reduce cost of multi-antenna users. Once the n-th antenna at user D_1 is selected, the channel for link D_1-BS is characterized by distribution $h_{D1S,n} \sim CN\left(0, \lambda_{1S,n}\right)$ with $(n = 1, \cdots, N)$. Similarly, we characterize the channel for the link D_2 to R (m-th antenna at user D_2 is decided to be transmitted) as $h_{D2R,m} \sim CN\left(0, \lambda_{2R,m}\right)$ with $(m = 1, \cdots, M)$, for link D_1-R, the channel distribution is $h_{D1R,n} \sim CN\left(0, \lambda_{1R,n}\right)$. For links associated with eavesdropper, links D_1-E, D_2 to E (the n-th antenna is selected at user D_1, the m-th antenna at user D_2) experience $h_{D1E,n} \sim CN\left(0, \lambda_{1E,n}\right)$, $h_{D2E,m} \sim CN\left(0, \lambda_{2E,m}\right)$, respectively.

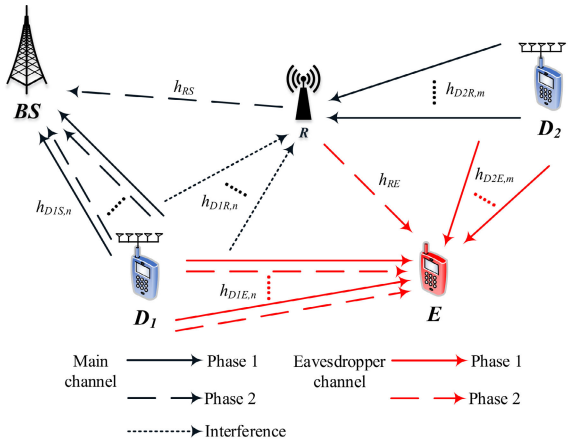

FIGURE 2. The extended case of multiple antennas at users.

A. PHASE 1

Similar (1), the received signal at BS from D_1 with multiple antenna in the first phase is given by

$$y_{D1,n-S}^{(p1)} = h_{D1S,n}\sqrt{\alpha_1 P}x_1 + \sigma_S. \tag{38}$$

The SINR at the BS to receive signal from multi-antenna user D_1 is given by

$$\gamma_{D1,n-S}^{(p1)} = \alpha_1\phi\left|h_{D1S,n}\right|^2. \tag{39}$$

The received signal at R in the first phase is given by

$$y_{R,nm}^{(p1)} = h_{D2R,m}\sqrt{\alpha_2 P}x_2 + h_{D1R,n}\sqrt{\alpha_1 P}x_1 + \sigma_R. \tag{40}$$

For multi-antenna user case, we only emphasize on the first case when $h_{D1R,n} > h_{D2R,m}$, R first decodes x_1 corresponding SINR as below [42]

$$\gamma_{R,1nm}^{(p1)} = \frac{\alpha_2\phi\left|h_{D2R,m}\right|^2}{\alpha_1\phi\left|\widetilde{h}_{D1R,n}\right|^2 + 1}, \tag{41}$$

where $\widetilde{h}_{D1R,n} \sim CN\left(0, \omega_1\lambda_{ip1,n}\right)$.

Case 2: If $h_{D1R,n} < h_{D2R,m}$ in the case G_2, R decodes the user symbol (i.e. x_2) subject to the better link quality by treating the user symbol (i.e. x_1) subject to the inferior link quality as noise [42]. The SINR of R is given by

$$\gamma_{R,2nm}^{(p1)} = \frac{\alpha_2\phi\left|h_{D2R,m}\right|^2}{\alpha_1\phi\left|h_{D1R,n}\right|^2 + 1}. \tag{42}$$

The received signal at E from multi-antenna users D_i in the first phase is given by

$$y_{E,nm}^{(p1)} = h_{D1E,n}\sqrt{\alpha_1 P}x_1 + h_{D2E,m}\sqrt{\alpha_2 P}x_2 + \sigma_E. \tag{43}$$

After PIC, the received SINR at eavesdropper to detect D_i's signals can be written as

$$\gamma_{Di,z-E}^{(p1)} = \alpha_i\phi_E\left|h_{DiE,z}\right|^2, \tag{44}$$

where $z = \{n; m\}$.

$$\begin{aligned}
\Theta_1 &= \Pr\left[|h_{D2R}|^2 > \frac{\phi_E|h_{D2E}|^2\left(\alpha_1\phi|h_{D1R}|^2 + 1\right)}{\phi}\right] \\
&= \int_0^\infty\int_0^\infty\left(1 - F_{|h_{D2R}|^2}\left(\frac{\phi_E x\left(\alpha_1\phi y + 1\right)}{\phi}\right)\right)f_{|h_{D2E}|^2}(x)f_{|h_{D1R}|^2}(y)\,dxdy \\
&= \frac{1}{\lambda_{2E}}\frac{1}{\lambda_{1R}}\int_0^\infty\int_0^\infty\exp\left(-\left(\frac{\phi_E\left(\alpha_1\phi y + 1\right)}{\phi\lambda_{2R}} + \frac{1}{\lambda_{2E}}\right)x\right)\exp\left(-\frac{y}{\lambda_{1R}}\right)dxdy \\
&= \frac{1}{\lambda_{1R}}\int_0^\infty\frac{\phi\lambda_{2R}}{\phi_E\alpha_1\phi\lambda_{2E}y + \phi_E\lambda_{2E} + \phi\lambda_{2R}}\exp\left(-\frac{y}{\lambda_{1R}}\right)dy \\
&= -\frac{\lambda_{2R}}{\alpha_1\phi_E\lambda_{2E}\lambda_{1R}}\exp\left(\Phi_4\right)\mathrm{Ei}\left(-\Phi_4\right).
\end{aligned} \tag{37}$$

B. PHASE 2

Similar (8), the received signal at BS from D_1 and R in the second phase is given by

$$y_{S,n}^{(p2)} = h_{D1S,n}\sqrt{\beta_1 P}y_1 + h_{RS}\sqrt{\beta_2 P}x_2 + \sigma_S. \quad (45)$$

Similar (9), we just consider details for the first case corresponding to $h_{D1R,n} > h_{RS}$, the BS first decodes y_1 and then x_2 using SIC. In particular, we examine the expressions of SINR for signals y_1, x_2 respectively as [42]

$$\gamma_{y_1,n}^{(p2)} = \frac{\beta_1\phi|h_{D1S,n}|^2}{\beta_2\phi|h_{RS}|^2 + 1}, \quad (46)$$

$$\gamma_{x_2,n}^{(p2)} = \frac{\beta_2\phi|h_{RS}|^2}{\beta_1\phi|\widetilde{h}_{D1S,n}|^2 + 1}, \quad (47)$$

where $\widetilde{h}_{D1S,n} \sim CN\left(0, \omega_2\lambda_{ip2,n}\right)$.

The received signal at E from R and D_1 with multi-antenna

$$y_{E,n}^{(p2)} = h_{D1E,n}\sqrt{\beta_1 P}y_1 + h_{RE}\sqrt{\beta_2 P}x_2 + \sigma_E. \quad (48)$$

After PIC, the received SINR at the eavesdropper to detect D_i's message can be written as

$$\gamma_{Di,z-E}^{(p2)} = \beta_i\phi_E|h_U|^2, \quad (49)$$

where $U = \{D1E, n; RE\}$.

The selected antenna can be achieved to strengthen uplink transmission from the user $D_1 \rightarrow$ BS and $D_2 \rightarrow R$ as [44]

$$n^* = \arg \underbrace{\max}_{n=1,\cdots,N} \left(|h_{D1S,n}|^2\right), \quad (50)$$

$$m^* = \arg \underbrace{\max}_{m=1,\cdots,M} \left(|h_{D2R,m}|^2\right). \quad (51)$$

The channel regarding selected antenna of D_1 and D_2 have PDF, and CDF respectively as [48]

$$F_{|h_T|^2}(x) = 1 - \sum_{z=1}^{Z}\binom{Z}{z}(-1)^{z-1}\exp\left(-\frac{zx}{\lambda_Q}\right), \quad (52)$$

$$f_{|h_T|^2}(x) = \sum_{z=1}^{Z}\binom{Z}{z}(-1)^{z-1}\frac{z}{\lambda_Q}\exp\left(-\frac{zx}{\lambda_Q}\right), \quad (53)$$

where $T = \{D1S, n^*; D2R, m^*\}$, $Q = \{1S, n; 2R, m\}$, $Z = \{N; M\}$, $z = \{n; m\}$.

C. ANALYSIS OF SOP

It is worth pointing out that selecting the optimal transmit antenna based on mentioned criteria lead to similar way in computing performance between user D_1 and user D_2, which expects that SOP performance depends on the number of antennas equipped at destinations D_1, D_2.

1) SOP OF D_1

Proposition 7: The closed-form expression of SOP for multi-antenna user D_1 can be expressed by

$$SOP_{D1}^{(n^*)} = 1 + \sum_{n=1}^{N}\sum_{r=1}^{N}\sum_{l=1}^{N}\sum_{t=1}^{N}\binom{N}{n}\binom{N}{r}\binom{N}{l}\binom{N}{t} \times (-1)^{n+r+l+t-4}\frac{r\phi\lambda_{1S,n}}{n\mu_1\phi_E\lambda_{1E,n}+r\phi\lambda_{1S,n}}\frac{t\lambda_{1S,n}}{l\mu_1\phi_E\beta_2\lambda_{1E,n}\lambda_{RS}} \times \exp\left(\bar{\lambda}_n\theta_n - \frac{n\overline{\mu_1}}{\alpha_1\phi\lambda_{1S,n}} - \frac{l\overline{\mu_1}}{\beta_1\phi\lambda_{1S,n}}\right)\mathrm{Ei}\left(-\bar{\lambda}_n\theta_n\right), \quad (54)$$

where $\bar{\lambda}_n = \frac{l\overline{\mu_1}\beta_2}{\beta_1\lambda_{1S,n}} + \frac{1}{\lambda_{RS}}$, $\theta_n = \frac{l\mu_1\phi_E\lambda_{1E,n}+t\phi\lambda_{1S,n}}{l\mu_1\phi_E\phi\beta_2\lambda_{1E,n}}$.

Proof: See Appendix E.

2) SOP OF D_2

We just focus on $G1$ case here. We omit another case since the case $G2$ can be proved in similar way. Then, the following proposition is provided to highlight benefits of multiple antennas design at users.

Proposition 8: The closed-form expression of SOP for $G_1 - D_2$ with M antennas can be expressed by

$$SOP_{D2}^{(G1,m^*)} = 1 - \sum_{m=1}^{M}\sum_{r=1}^{M}\sum_{l=1}^{N}\sum_{t=1}^{N}\binom{M}{m}\binom{M}{r}\binom{N}{l}\binom{N}{t} \times (-1)^{m+r+l+t-4}\frac{rl\lambda_{2R,m}}{m\mu_2\alpha_1\phi_E\omega_1\lambda_{ip1,n}\lambda_{2E,m}} \frac{t\lambda_{RS}}{\mu_2\beta_1\phi_E\omega_2\lambda_{ip2,n}\lambda_{RE}} \times \exp\left(\psi_{1,m}\delta_{1,m} - \frac{m\overline{\mu_2}}{\alpha_2\phi\lambda_{2R,m}} + \psi_2\delta_{2,m} - \frac{\overline{\mu_2}}{\beta_2\phi\lambda_{RS}}\right) \times \mathrm{Ei}\left(-\psi_{1,m}\delta_{1,m}\right)\mathrm{Ei}\left(-\psi_2\delta_{2,m}\right), \quad (55)$$

where $\psi_{1,m} = \frac{m\mu_2\phi_E\lambda_{2E,m}+r\phi\lambda_{2R,m}}{m\mu_2\alpha_1\phi\phi_E\lambda_{2E,m}}$, $\delta_{1,m} = \frac{m\overline{\mu_2}\alpha_1}{\alpha_2\lambda_{2R,m}} + \frac{l}{\omega_1\lambda_{ip1,n}}$, $\delta_{2,m} = \frac{\overline{\mu_2}\beta_1}{\beta_2\lambda_{RS}} + \frac{t}{\omega_2\lambda_{ip2,n}}$.

Proof: See Appendix F.

D. ANALYSIS OF SPSC

1) SPSC OF D_1

Proposition 9: The closed-form expression of SPSC for D_1 with N antennas can be expressed by

$$SPSC_{D1}^{(n^*)} = -\sum_{n=1}^{N}\sum_{r=1}^{N}\sum_{l=1}^{N}\sum_{t=1}^{N}\binom{N}{n}\binom{N}{r}\binom{N}{l}\binom{N}{t} \times (-1)^{n+r+l+t-4}\frac{r\phi\lambda_{1S,n}}{n\phi_E\lambda_{1E,n} + r\phi\lambda_{1S,n}}\frac{t\lambda_{1S,n}}{l\beta_2\phi_E\lambda_{1E,n}\lambda_{RS}} \times \exp\left(\Phi_{1,n}\right)\mathrm{Ei}\left(-\Phi_{1,n}\right), \quad (56)$$

where $\Phi_{1,n} = \frac{l\phi_E\lambda_{1E,n}+t\phi\lambda_{1S,n}}{l\beta_2\phi_E\phi\lambda_{1E,n}\lambda_{RS}}$.

Proof: See Appendix G.

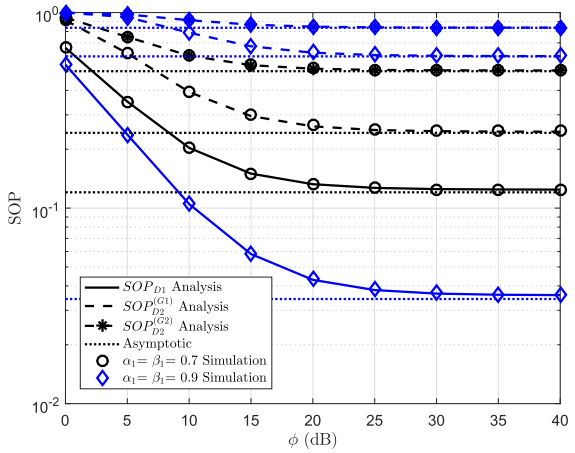

FIGURE 3. SOP vs transmit SNR with different $\alpha_1 = \beta_1$ [51] ($R_{D1} = R_{D2} = 0.2$ (bps/Hz), $\lambda_{1S} = \lambda_{RS} = \lambda_{1R} = \lambda_{2R} = 1$ [43], $\lambda_{ip1} = \lambda_{ip2} = 1$, $\lambda_{1E} = \lambda_{2E} = \lambda_{RE} = 0.01$, $\omega = \omega_1 = \omega_2 = 0.2$ [52], $\phi_E = 1$ (dB)).

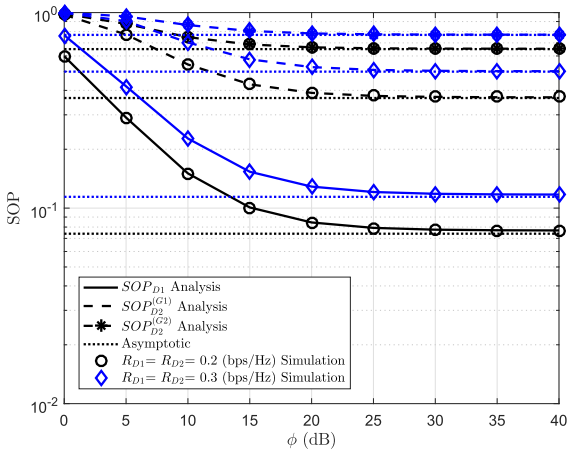

FIGURE 4. SOP vs transmit SNR with different $R_{D1} = R_{D2}$ ($\alpha_1 = \beta_1 = 0.8$ [51], $\alpha_2 = \beta_2 = 0.2$, $\lambda_{1S} = \lambda_{RS} = \lambda_{1R} = \lambda_{2R} = 1$ [43], $\lambda_{ip1} = \lambda_{ip2} = 1$, $\lambda_{1E} = \lambda_{2E} = \lambda_{RE} = 0.01$, $\omega = \omega_1 = \omega_2 = 0.2$ [52], $\phi_E = 1$ (dB)).

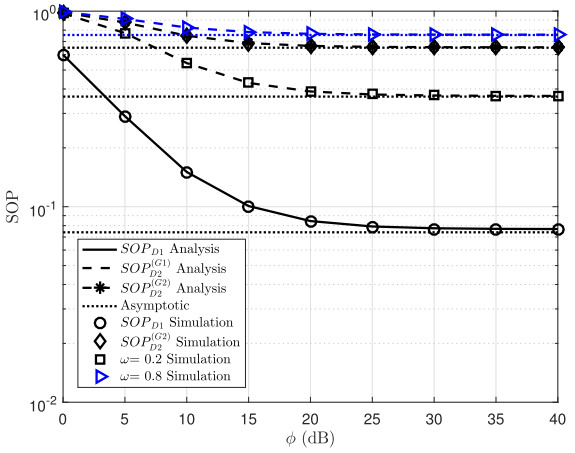

FIGURE 5. SOP vs transmit SNR with different $\omega = \omega_1 = \omega_2$ ($\alpha_1 = \beta_1 = 0.8$ [51], $\alpha_2 = \beta_2 = 0.2$, $R_{D1} = R_{D2} = 0.2$ (bps/Hz), $\lambda_{1S} = \lambda_{RS} = \lambda_{1R} = \lambda_{2R} = 1$ [43], $\lambda_{ip1} = \lambda_{ip2} = 1$, $\lambda_{1E} = \lambda_{2E} = \lambda_{RE} = 0.01$, $\phi_E = 1$ (dB)).

2) SPSC OF D_2

Proposition 10: The closed-form expression of SPSC for multi-antenna user D_2 (case $G1$ only) can be formulated by

$$SPSC_{D2}^{(G1,m^*)} = \sum_{m=1}^{M}\sum_{r=1}^{M}\sum_{l=1}^{N}\sum_{t=1}^{N}\binom{M}{m}\binom{M}{r}\binom{N}{l}\binom{N}{t} \times(-1)^{m+r+l+t-4}\frac{rl\lambda_{2R,m}}{m\alpha_1\phi_E\lambda_{2E,m}\omega_1\lambda_{ip1,n}}\frac{t\lambda_{RS}}{\beta_1\phi_E\lambda_{RE}\omega_2\lambda_{ip2,n}} \times \exp\left(\Phi_{2,m}+\Phi_{3,m}\right)\mathrm{Ei}\left(-\Phi_{2,m}\right)\mathrm{Ei}\left(-\Phi_{3,m}\right), \quad (57)$$

where $\Phi_{2,m} = \frac{lm\phi_E\lambda_{2E,m}+lr\phi\lambda_{2R,m}}{m\alpha_1\phi_E\lambda_{2E,m}\omega_1\lambda_{ip1,n}}$, $\Phi_{3,m} = \frac{t\phi_E\lambda_{RE}+t\phi\lambda_{RS}}{\beta_1\phi_E\lambda_{RE}\omega_2\lambda_{ip2,n}}$.

Proof: See Appendix H.

Remark 3: As discussed earlier, two single antenna users experience different SOP as well as SPSC which mainly depends on power allocation factors, and channel gains. By contrast, multi-antenna users exhibit improved SOP and SPSC performance as expected, shown in (54), (54), (56) *and* (57). *The uplink communication tasks in the context of NOMA strategy shows more complicated expressions of secure performance. However, even though similar setup of end-to-end SINR and target transmission rate, and the selection criterion is indeed a combination of the best transmit antennas at two multi-antenna users to produce an improvement. Unfortunately, a challenging issue may arises: how could the antenna can be jointly selected so that the optimal performance of such system is enhanced? To tackle this problem, we develop numerical experiment to evaluate antenna parameters N, M to secure performance.*

VI. SIMULATION RESULTS

In this section, we conduct numerical simulation by run 10^6 iterations for Monte-Carlo simulation. Main parameters are provided in each figure.

In Fig. 3, we first analyze the SOP secrecy performance versus the transmit SNR ϕ at the BS over different power allocation factors when $\alpha_1 = \beta_1$, in which the asymptotic lines are included to show the lower bound of these SOP curves. As can be observed from the curves and the corresponding markers, the Monte-Carlo results are matched tightly with the analytical results and such good agreement validates the accuracy of our analytical results. As for the comparison of the SOPs, the simulation results exhibit the best case for user D_1 since the high power factor is allocated to it. We observe that the SOP is a monotonically decreasing function of ϕ, since the SINRs depend on ϕ. It's obvious that the change in $\alpha_1 = \beta_1$ from 0.9 to 0.7 leads to deduction of SOP performance. Thus, the secrecy performance can be improved at the cost of reliable performance by controlling α_1 and β_1.

Fig. 4 shows the similar trends of SOP performance of two users by changing the target rates, R_{D1}, R_{D2}. Since formulas of SOP depend on these values of R_{D1}, R_{D2}, the lower requiblack target rates result in a better SOP performance.

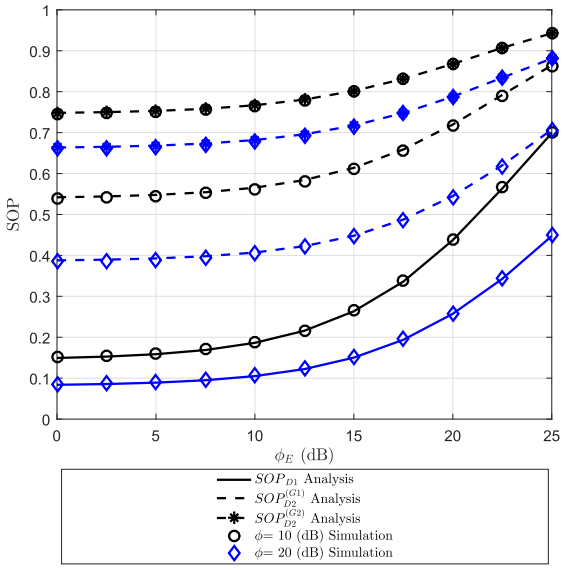

FIGURE 6. SOP vs transmit ϕ_E with different SNR ($\alpha_1 = \beta_1 = 0.8$ [51], $\alpha_2 = \beta_2 = 0.2$, $R_{D1} = R_{D2} = 0.2$ (bps/Hz), $\lambda_{1S} = \lambda_{RS} = \lambda_{1R} = \lambda_{2R} = 1$ [43], $\lambda_{ip1} = \lambda_{ip2} = 1$, $\lambda_{1E} = \lambda_{2E} = \lambda_{RE} = 0.01$, $\omega = \omega_1 = \omega_2 = 0.2$ [52]).

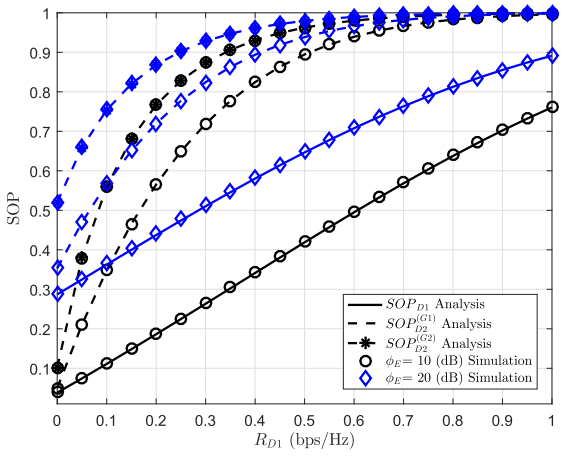

FIGURE 7. SOP vs transmit $R_{D1} = R_{D2}$ with different ϕ_E ($\alpha_1 = \beta_1 = 0.8$ [51], $\alpha_2 = \beta_2 = 0.2$, $\lambda_{1S} = \lambda_{RS} = \lambda_{1R} = \lambda_{2R} = 1$ [43], $\lambda_{ip1} = \lambda_{ip2} = 1$, $\lambda_{1E} = \lambda_{2E} = \lambda_{RE} = 0.01$, $\omega = \omega_1 = \omega_2 = 0.2$ [52], $\phi = 10$ (dB)).

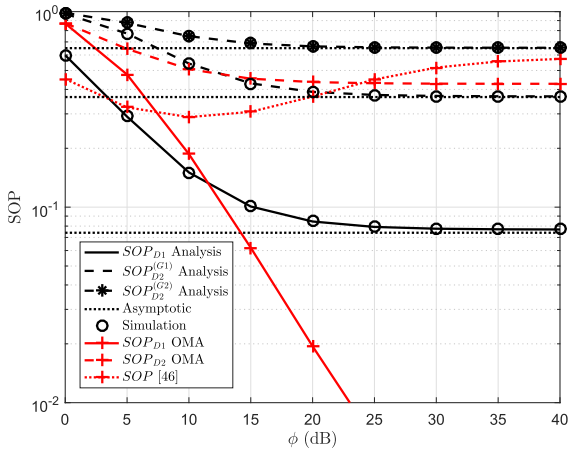

FIGURE 8. SOP vs transmit SNR with OMA and [46] ($\alpha_1 = \beta_1 = 0.8$ [51], $\alpha_2 = \beta_2 = 0.2$, $R_{D1} = R_{D2} = 0.2$ (bps/Hz), $\lambda_{1S} = \lambda_{RS} = \lambda_{1R} = \lambda_{2R} = 1$ [43], $\lambda_{ip1} = \lambda_{ip2} = 1$, $\lambda_{1E} = \lambda_{2E} = \lambda_{RE} = 0.01$, $\omega = \omega_1 = \omega_2 = 0.2$ [52], $\phi_E = 1$ (dB)).

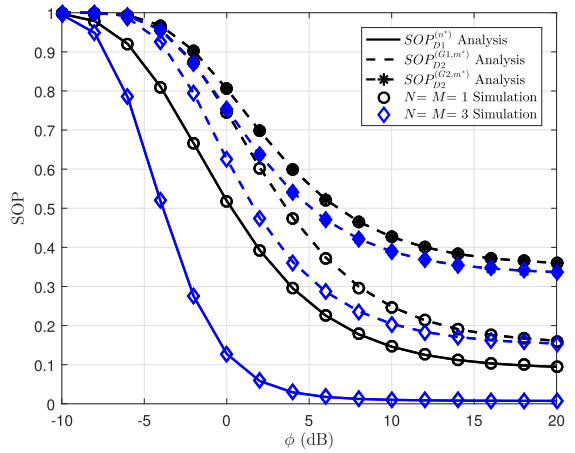

FIGURE 9. SOP for multi-antenna user vs transmit SNR with different $N = M$ ($\alpha_1 = \beta_1 = 0.7$ [51], $\alpha_2 = \beta_2 = 0.1$, $R_{D1} = R_{D2} = 0.2$ (bps/Hz), $\lambda_{1S,n} = \lambda_{RS} = \lambda_{1R,n} = \lambda_{2R,m} = 1$ [43], $\lambda_{ip1,n} = \lambda_{ip2,n} = 1$, $\lambda_{1E,n} = \lambda_{2E,m} = \lambda_{RE} = 0.01$, $\omega = \omega_1 = \omega_2 = 0.2$ [52], $\phi_E = 10$ (dB)).

It is confirmed that the lower bound of SOP is matched with the exact SOP values at high SNR regime, i.e. $\phi = 40$ (dB).

The impact of the level of imperfect SIC at user D_2 can be seen clearly as Fig. 5. Once we set $\omega = 0.8$, it causes a significant reduction in the SOP. Further, the channel conditions reported in cases G_1 and G_2 also show performance gaps for consideration on performance of user D_2. Since formulas of SOP depend on the transmit SNR, and hence high SNR leads to significant improvement on SOP performance.

As observed from expressions of SOP metric in Fig. 6, for example (25) reports that the SOP performance will become worse if the SNR of the eavesdropper increases. We can confirm such result as seen in Fig. 6. The impact of transmit SNR at the base station also contribute to improving performance in this circumstance. Further, ϕ_E in the range from 15 (dB) to 25 (dB) results in significant variations of SOP.

In Fig. 7, as further observation from expressions of SOP metric, for example (25) indicates that the target rates are main parameter to limit the performance of SOP. The curves of SOP approach to 1 when the target rates $R_{D1} = R_{D2} = 0.8$ (bps/Hz) except for the case of user D_1. The performance gaps between the two users still exist. It can be explained that the power allocation factors make crucial influence to SINR and corresponding SOP performance. Fig. 8 further provides the comparison between NOMA, the work in [46] and OMA cases.

Fig. 9 reveals the impact of antenna configurations at two users on the secure system performance. The big gap for user D_1 for two cases of transmit antennas $N = M = 1$ and $N = M = 3$ as can be observed from 9, while SOP

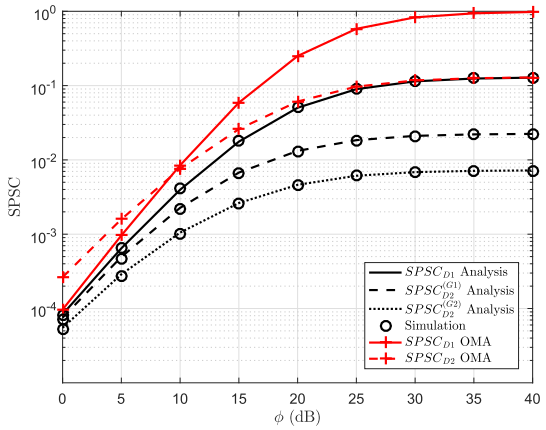

FIGURE 10. SPSC vs transmit SNR with different OMA ($\alpha_1 = \beta_1 = 0.8$ [51], $\alpha_2 = \beta_2 = 0.2$, $\lambda_{1S} = \lambda_{RS} = \lambda_{1R} = \lambda_{2R} = 1$ [43], $\lambda_{ip1} = \lambda_{ip2} = 1$, $\lambda_{1E} = \lambda_{2E} = \lambda_{RE} = 0.01$, $\omega = \omega_1 = \omega_2 = 0.2$ [52], $\phi_E = 40$ (dB)).

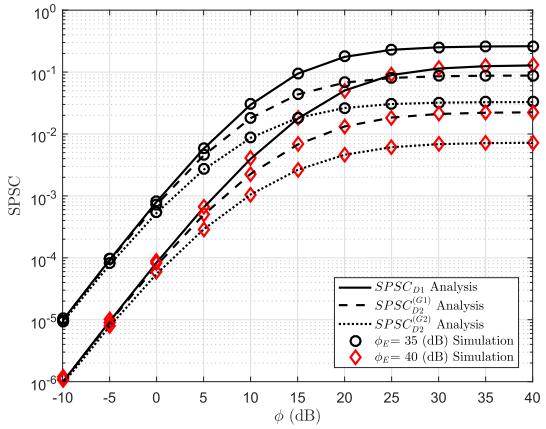

FIGURE 11. SPSC vs transmit SNR with different ϕ_E ($\alpha_1 = \beta_1 = 0.8$ [51], $\alpha_2 = \beta_2 = 0.2$, $\lambda_{1S} = \lambda_{RS} = \lambda_{1R} = \lambda_{2R} = 1$, $\lambda_{ip1} = \lambda_{ip2} = 1$, $\lambda_{1E} = \lambda_{2E} = \lambda_{RE} = 0.01$, $\omega = \omega_1 = \omega_2 = 0.2$ [52]).

performance of user D_1 just slightly relies on the antenna configuration. The main reason is that decoding signal procedure at the BS for user D_1 is more complicated since it belongs to processing at both transmission hops. On the other hand, the SOP performance has also floor at high SNR region which indicates that more antennas at users only contribute to improvement at low SNR region which more system parameters with higher weight compared to ϕ.

Then, Fig. 10 shows the increase in the SPSC performance when the SNR at the BS increases ϕ. The performance gap between the two users is still observable in this figure. We provide more comparisons on OMA as well. In this case, D_1 is reported as best case except for OMA case. It is obvious that ϕ_E results in the deduction of SPSC in Fig. 11. We also know from the calculated expression that SPSC is a monotonically increasing function of ϕ. Similarly, as shown in Fig. 12, the impact of power allocation factors is small if we compare the two cases of $\alpha_1 = \beta_1 = 0.8$ and $\alpha_1 = \beta_1 = 0.2$.

Furthermore, the impact of imperfect SIC on SPSC can be seen clearly in Fig. 13. When ϕ_E changes from 35 to 40, the SPSC performance of user D_2 is affected significantly. Other trends of such secure performance metric are similar as

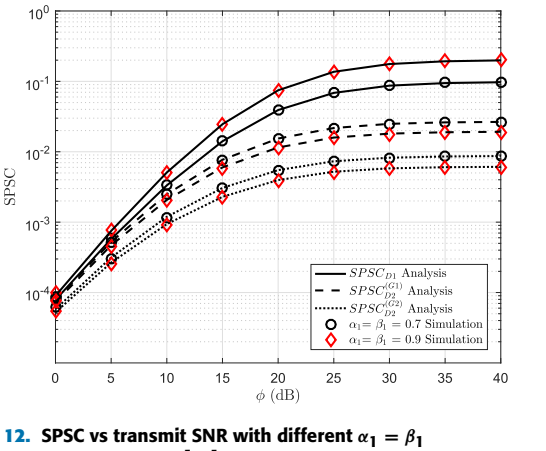

FIGURE 12. SPSC vs transmit SNR with different $\alpha_1 = \beta_1$ ($\lambda_{1S} = \lambda_{RS} = \lambda_{1R} = \lambda_{2R} = 1$ [43], $\lambda_{ip1} = \lambda_{ip2} = 1$, $\lambda_{1E} = \lambda_{2E} = \lambda_{RE} = 0.01$, $\omega = \omega_1 = \omega_2 = 0.2$ [52], $\phi_E = 40$ (dB)).

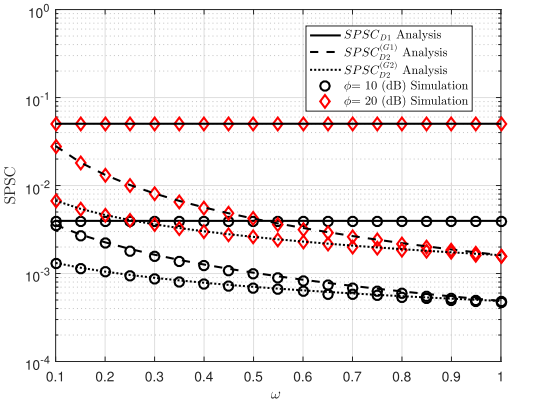

FIGURE 13. SPSC vs transmit SNR with different $\omega = \omega_1 = \omega_2$ ($\alpha_1 = \beta_1 = 0.8$ [51], $\alpha_2 = \beta_2 = 0.2$, $\lambda_{1S} = \lambda_{RS} = \lambda_{1R} = \lambda_{2R} = 1$ [43], $\lambda_{ip1} = \lambda_{ip2} = 1$, $\lambda_{1E} = \lambda_{2E} = \lambda_{RE} = 0.01$, $\phi_E = 40$ (dB)).

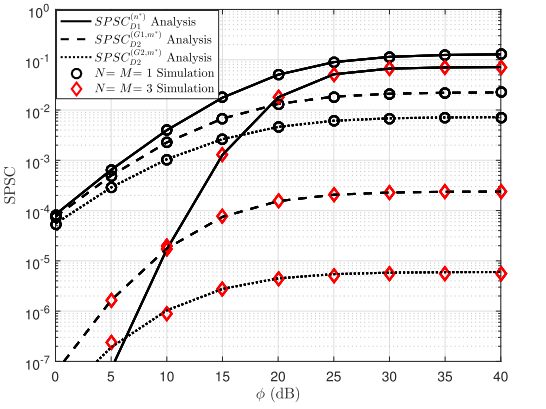

FIGURE 14. SPSC for multiple antenna vs transmit SNR with different $N = M$ ($\alpha_1 = \beta_1 = 0.8$ [51], $\alpha_2 = \beta_2 = 0.2$, $\lambda_{1S,n} = \lambda_{RS} = \lambda_{1R,n} = \lambda_{2R,m} = 1$ [43], $\lambda_{ip1,n} = \lambda_{ip2,n} = 1$, $\lambda_{1E,n} = \lambda_{2E,m} = \lambda_{RE} = 0.01$, $\omega = \omega_1 = \omega_2 = 0.2$ [52], $\phi_E = 40$ (dB)).

previous figures. Similarly, Fig. 14 compares SPSC for two cases of antenna configuration, $N = M = 1$ and $N = M = 3$.

VII. CONCLUSION

In this paper, we studied the secrecy performance of an uplink NOMA for single antenna and multiple antennas users cases. We consider the uplink transmission scenario where users are

classified based on their locations around the serving base station in the presence of an eavesdropper. We also analyzed the PLS performances in terms of SOP and SPSC. Such uplink NOMA transmission proves reliability since there are two kinds of links from user ends to the base station. A group of two NOMA users is adopted to have a tractable analysis since the interference from other groups is neglected. Based on the proposed model, the closed-form expressions of SOP and SPSC are derived for characterizing the systems' reliability performance and secrecy performance. Additionally, we provide the main parameters which explicitly capture the reliability performance and secrecy performance of the network. It's proved that the performance gaps of two users in terms of SOP and SPSC can be improved by varying power allocation factors and channel conditions. It is worth mentioning that the results in this study are primarily theoretically oriented and offer a useful theoretical guidelines for uplink NOMA transmission in cellular systems.

APPENDIX A
PROOF OF PROPOSITION 1

From (20), the SOP of D_1 can written by

$$SOP_{D1} = 1 - \underbrace{\Pr\left[\frac{1+\gamma_{D1-S}^{(p1)}}{1+\gamma_{D1-E}^{(p1)}} \geq \mu_1\right]}_{A_1} \times \underbrace{\Pr\left[\frac{1+\gamma_{y_1}^{(p2)}}{1+\gamma_{D1-E}^{(p2)}} < \mu_1\right]}_{A_2}. \quad \text{(A.1)}$$

From (A.1), A_1 can be calculated as

$$\begin{aligned} A_1 &= \Pr\left[\gamma_{D1-S}^{(p1)} \geq \overline{\mu_1} + \mu_1\gamma_{D1-E}^{(p1)}\right] \\ &= \Pr\left[|h_{D1S}|^2 \geq \frac{\overline{\mu_1} + \mu_1\alpha_1\phi_E|h_{D1E}|^2}{\alpha_1\phi}\right] \\ &= \int_0^\infty \left(1 - F_{|h_{D1S}|^2}\left(\frac{\overline{\mu_1} + \mu_1\alpha_1\phi_E x}{\alpha_1\phi}\right)\right) \\ &\quad \times f_{|h_{D1E}|^2}(x)\,dx \\ &= \frac{1}{\lambda_{1E}}\exp\left(-\frac{\overline{\mu_1}}{\alpha_1\phi\lambda_{1S}}\right) \\ &\quad \times \int_0^\infty \exp\left(-\left(\frac{\mu_1\phi_E}{\phi\lambda_{1S}} + \frac{1}{\lambda_{1E}}\right)x\right)dx \\ &= \frac{\phi\lambda_{1S}}{\mu_1\phi_E\lambda_{1E} + \phi\lambda_{1S}}\exp\left(-\frac{\overline{\mu_1}}{\alpha_1\phi\lambda_{1S}}\right). \end{aligned} \quad \text{(A.2)}$$

From (A.1), A_2 can be calculated as (A.3), shown at the bottom of the next page.

Based on [45, Eq. (3.352.4)] and applying some polynomial expansion manipulations, A_2 is given by

$$A_2 = -\frac{\lambda_{1S}}{\mu_1\phi_E\beta_2\lambda_{1E}\lambda_{RS}}\exp\left(\bar{\lambda}\theta - \frac{\overline{\mu_1}}{\beta_1\phi\lambda_{1S}}\right)\mathrm{Ei}\left(-\bar{\lambda}\theta\right), \quad \text{(A.4)}$$

where $\bar{\lambda} = \frac{\overline{\mu_1}\beta_2}{\beta_1\lambda_{1S}} + \frac{1}{\lambda_{RS}}$, $\theta = \frac{\mu_1\phi_E\lambda_{1E}+\phi\lambda_{1S}}{\mu_1\phi_E\phi\beta_2\lambda_{1E}}$.

Substituting (A.2) and (A.4) into (A.1), we can obtain (21). The proof is completed.

APPENDIX B
PROOF OF PROPOSITION 2

From (22), B_1 can be calculated as (B.1), shown at the bottom of the next page.

Based on [45, Eq. (3.352.4)] and applying some polynomial expansion manipulations, B_1 is given by

$$B_1 = -\frac{\lambda_{2R}}{\mu_2\alpha_1\phi_E\omega_1\lambda_{ip1}\lambda_{2E}}\exp\left(\psi_1\delta_1 - \frac{\overline{\mu_2}}{\alpha_2\phi\lambda_{2R}}\right) \times \mathrm{Ei}\left(-\psi_1\delta_1\right), \quad \text{(B.2)}$$

where $\psi_1 = \frac{\mu_2\phi_E\lambda_{2E}+\phi\lambda_{2R}}{\mu_2\alpha_1\phi\phi_E\lambda_{2E}}$, $\delta_1 = \frac{\overline{\mu_2}\alpha_1}{\alpha_2\lambda_{2R}} + \frac{1}{\omega_1\lambda_{ip1}}$.

Next, B_2 can be calculated as (B.3), shown at the bottom of the next page.

Similar B_1, based on [45, Eq. (3.352.4)] and applying some polynomial expansion manipulations, B_2 is given by

$$B_2 = -\frac{\lambda_{RS}}{\mu_2\beta_1\phi_E\omega_2\lambda_{ip2}\lambda_{RE}}\exp\left(\psi_2\delta_2 - \frac{\overline{\mu_2}}{\beta_2\phi\lambda_{RS}}\right) \times \mathrm{Ei}\left(-\psi_2\delta_2\right), \quad \text{(B.4)}$$

where $\psi_2 = \frac{\mu_2\phi_E\lambda_{RE}+\phi\lambda_{RS}}{\mu_2\beta_1\phi_E\phi\lambda_{RE}}$, $\delta_2 = \frac{\overline{\mu_2}\beta_1}{\beta_2\lambda_{RS}} + \frac{1}{\omega_2\lambda_{ip2}}$.

Substituting (B.2) and (B.4) into (22), we can obtain (23). The proof is completed.

APPENDIX C
PROOF OF PROPOSITION 3

From (31), we can express Q_1 as

$$\begin{aligned} Q_1 &= \Pr\left[|h_{D1S}|^2 > \frac{\phi_E|h_{D1E}|^2}{\phi}\right] \\ &= \frac{1}{\lambda_{1E}}\int_0^\infty \exp\left(-\left(\frac{\phi_E}{\phi\lambda_{1S}} + \frac{1}{\lambda_{1E}}\right)x\right)dx \\ &= \frac{\phi\lambda_{1S}}{\phi_E\lambda_{1E} + \phi\lambda_{1S}}. \end{aligned} \quad \text{(C.1)}$$

Further, Q_2 can be calculated as

$$\begin{aligned} Q_2 &= \Pr\left[|h_{D1S}|^2 > \frac{\phi_E|h_{D1E}|^2\left(\beta_2\phi|h_{RS}|^2 + 1\right)}{\phi}\right] \\ &= \int_0^\infty\int_0^\infty \left(1 - F_{|h_{D1S}|^2}\left(\frac{\phi_E x\left(\beta_2\phi y + 1\right)}{\phi}\right)\right) \\ &\quad \times f_{|h_{D1E}|^2}(x) f_{|h_{RS}|^2}(y)\,dxdy \\ &= \int_0^\infty\int_0^\infty \exp\left(-\frac{\phi_E x\left(\beta_2\phi y + 1\right)}{\phi\lambda_{1S}}\right)\frac{1}{\lambda_{1E}}\exp\left(-\frac{x}{\lambda_{1E}}\right) \end{aligned}$$

$$\times \frac{1}{\lambda_{RS}} \exp\left(-\frac{y}{\lambda_{RS}}\right) dxdy$$
$$= \frac{1}{\lambda_{1E}} \frac{1}{\lambda_{RS}} \int_0^\infty \int_0^\infty \exp\left(-\left(\frac{\phi_E\left(\beta_2\phi y+1\right)}{\phi\lambda_{1S}}+\frac{1}{\lambda_{1E}}\right)x\right)$$
$$\times \exp\left(-\frac{y}{\lambda_{RS}}\right) dxdy$$
$$= \frac{1}{\lambda_{RS}} \int_0^\infty \frac{\phi\lambda_{1S}}{\phi_E\beta_2\phi\lambda_{1E}y+\beta_1\phi_E\lambda_{1E}+\phi\lambda_{1S}} \exp\left(-\frac{y}{\lambda_{RS}}\right) dy. \quad \text{(C.2)}$$

Based on [45, Eq. (3.352.4)] and applying some polynomial expansion manipulations, Q_2 is written as

$$Q_2 = -\frac{\lambda_{1S}}{\beta_2\phi_E\lambda_{1E}\lambda_{RS}} \exp\left(\Phi_1\right) \mathrm{Ei}\left(-\Phi_1\right), \quad \text{(C.3)}$$

where $\Phi_1 = \frac{\phi_E\lambda_{1E}+\phi\lambda_{1S}}{\beta_2\phi_E\phi\lambda_{1E}\lambda_{RS}}$.

The expected result can be obtained as plugging (C.1) and (C.3) into (31).

It is the end of the proof.

$$A_2 = \Pr\left[\gamma_{y_1}^{(p2)} \geq \overline{\mu_1} + \mu_1\gamma_{D1-E}^{(p2)}\right]$$
$$= \Pr\left[\frac{\beta_1\phi|h_{D1S}|^2}{\beta_2\phi|h_{RS}|^2+1} \geq \overline{\mu_1} + \mu_1\beta_1\phi_E|h_{D1E}|^2\right]$$
$$= \Pr\left[|h_{D1S}|^2 \geq \frac{\left(\overline{\mu_1}+\mu_1\beta_1\phi_E|h_{D1E}|^2\right)\left(\beta_2\phi|h_{RS}|^2+1\right)}{\beta_1\phi}\right]$$
$$= \int_0^\infty \int_0^\infty \left(1 - F_{|h_{D1S}|^2}\left(\frac{\left(\overline{\mu_1}+\mu_1\beta_1\phi_E x\right)\left(\beta_2\phi y+1\right)}{\beta_1\phi}\right)\right) f_{|h_{D1E}|^2}(x) f_{|h_{RS}|^2}(y)\, dxdy$$
$$= \frac{1}{\lambda_{1E}} \frac{1}{\lambda_{RS}} \exp\left(-\frac{\overline{\mu_1}}{\beta_1\phi\lambda_{1S}}\right) \int_0^\infty \int_0^\infty \exp\left(-\left(\frac{\mu_1\phi_E\beta_2\phi y+\mu_1\phi_E}{\phi\lambda_{1S}}+\frac{1}{\lambda_{1E}}\right)x\right) \exp\left(-\left(\frac{\overline{\mu_1}\beta_2}{\beta_1\lambda_{1S}}+\frac{1}{\lambda_{RS}}\right)y\right) dxdy$$
$$= \frac{1}{\lambda_{RS}} \exp\left(-\frac{\overline{\mu_1}}{\beta_1\phi\lambda_{1S}}\right) \int_0^\infty \frac{\phi\lambda_{1S}}{\mu_1\phi_E\beta_2\phi\lambda_{1E}y+\mu_1\phi_E\lambda_{1E}+\phi\lambda_{1S}} \exp\left(-\left(\frac{\overline{\mu_1}\beta_2}{\beta_1\lambda_{1S}}+\frac{1}{\lambda_{RS}}\right)y\right) dy. \quad \text{(A.3)}$$

$$B_1 = \Pr\left[\gamma_{R,1}^{(p1)} \geq \overline{\mu_2} + \mu_2\gamma_{D2-E}^{(p1)}\right]$$
$$= \Pr\left[|h_{D2R}|^2 \geq \frac{\left(\overline{\mu_2}+\mu_2\alpha_2\phi_E|h_{D2E}|^2\right)\left(\alpha_1\phi\left|\widetilde{h}_{D1R}\right|^2+1\right)}{\alpha_2\phi}\right]$$
$$= \int_0^\infty \int_0^\infty \left(1 - F_{|h_{D2R}|^2}\left(\frac{\left(\overline{\mu_2}+\mu_2\alpha_2\phi_E x\right)\left(\alpha_1\phi y+1\right)}{\alpha_2\phi}\right)\right) f_{|h_{D2E}|^2}(x) f_{\left|\widetilde{h}_{D1R}\right|^2}(y)\, dxdy$$
$$= \int_0^\infty \int_0^\infty \exp\left(-\frac{\left(\overline{\mu_2}+\mu_2\alpha_2\phi_E x\right)\left(\alpha_1\phi y+1\right)}{\alpha_2\phi\lambda_{2R}}\right) \frac{1}{\lambda_{2E}} \exp\left(-\frac{x}{\lambda_{2E}}\right) \frac{1}{\omega_1\lambda_{ip1}} \exp\left(-\frac{y}{\omega_1\lambda_{ip1}}\right) dxdy$$
$$= \frac{1}{\lambda_{2E}} \frac{1}{\omega_1\lambda_{ip1}} \exp\left(-\frac{\overline{\mu_2}}{\alpha_2\phi\lambda_{2R}}\right) \int_0^\infty \int_0^\infty \exp\left(-\left(\frac{\mu_2\alpha_1\phi\phi_E y+\mu_2\phi_E}{\phi\lambda_{2R}}+\frac{1}{\lambda_{2E}}\right)x\right) \exp\left(-\left(\frac{\overline{\mu_2}\alpha_1}{\alpha_2\lambda_{2R}}+\frac{1}{\omega_1\lambda_{ip1}}\right)y\right) dxdy$$
$$= \frac{1}{\omega_1\lambda_{ip1}} \exp\left(-\frac{\overline{\mu_2}}{\alpha_2\phi\lambda_{2R}}\right) \int_0^\infty \frac{\phi\lambda_{2R}}{\mu_2\alpha_1\phi\phi_E\lambda_{2E}y+\mu_2\phi_E\lambda_{2E}+\phi\lambda_{2R}} \exp\left(-\left(\frac{\overline{\mu_2}\alpha_1}{\alpha_2\lambda_{2R}}+\frac{1}{\omega_1\lambda_{ip1}}\right)y\right) dy. \quad \text{(B.1)}$$

$$B_2 = \Pr\left[\gamma_{x_2}^{(p2)} \geq \overline{\mu_2} + \mu_2\gamma_{D2-E}^{(p2)}\right]$$
$$= \Pr\left[|h_{RS}|^2 \geq \frac{\left(\overline{\mu_2}+\mu_2\beta_2\phi_E|h_{RE}|^2\right)\left(\beta_1\phi\left|\widetilde{h}_{D1S}\right|^2+1\right)}{\beta_2\phi}\right]$$
$$= \int_0^\infty \int_0^\infty \left(1 - F_{|h_{RS}|^2}\left(\frac{\left(\overline{\mu_2}+\mu_2\beta_2\phi_E x\right)\left(\beta_1\phi y+1\right)}{\beta_2\phi}\right)\right) f_{|h_{RE}|^2}(x) f_{\left|\widetilde{h}_{D1S}\right|^2}(y)\, dxdy$$
$$= \int_0^\infty \int_0^\infty \exp\left(-\frac{\left(\overline{\mu_2}+\mu_2\beta_2\phi_E x\right)\left(\beta_1\phi y+1\right)}{\beta_2\phi\lambda_{RS}}\right) \frac{1}{\lambda_{RE}} \exp\left(-\frac{x}{\lambda_{RE}}\right) \frac{1}{\omega_2\lambda_{ip2}} \exp\left(-\frac{y}{\omega_2\lambda_{ip2}}\right) dxdy$$
$$= \frac{1}{\lambda_{RE}} \frac{1}{\omega_2\lambda_{ip2}} \exp\left(-\frac{\overline{\mu_2}}{\beta_2\phi\lambda_{RS}}\right) \int_0^\infty \int_0^\infty \exp\left(-\left(\frac{\mu_2\beta_1\phi_E\phi y+\mu_2\phi_E}{\phi\lambda_{RS}}+\frac{1}{\lambda_{RE}}\right)x\right) \exp\left(-\left(\frac{\overline{\mu_2}\beta_1}{\beta_2\lambda_{RS}}+\frac{1}{\omega_2\lambda_{ip2}}\right)y\right) dxdy$$
$$= \frac{1}{\omega_2\lambda_{ip2}} \exp\left(-\frac{\overline{\mu_2}}{\beta_2\phi\lambda_{RS}}\right) \int_0^\infty \frac{\phi\lambda_{RS}}{\mu_2\beta_1\phi_E\phi\lambda_{RE}y+\mu_2\phi_E\lambda_{RE}+\phi\lambda_{RS}} \exp\left(-\left(\frac{\overline{\mu_2}\beta_1}{\beta_2\lambda_{RS}}+\frac{1}{\omega_2\lambda_{ip2}}\right)y\right) dy. \quad \text{(B.3)}$$

APPENDIX D
PROOF OF PROPOSITION 4

With the help of (33), W_1 is given as

$$\begin{aligned}
W_1 &= \Pr\left[|h_{D2R}|^2 > \frac{\phi_E|h_{D2E}|^2\left(\alpha_1\phi|\widetilde{h}_{D1R}|^2+1\right)}{\phi}\right] \\
&= \int_0^\infty\int_0^\infty\left(1-F_{|h_{D2R}|^2}\left(\frac{\phi_E x\left(\alpha_1\phi y+1\right)}{\phi}\right)\right)f_{|h_{D2E}|^2}(x) \\
&\quad\times f_{|\widetilde{h}_{D1R}|^2}(y)\,dxdy \\
&= \int_0^\infty\int_0^\infty \exp\left(-\frac{\phi_E x\left(\alpha_1\phi y+1\right)}{\phi\lambda_{2R}}\right)\frac{1}{\lambda_{2E}}\exp\left(-\frac{x}{\lambda_{2E}}\right) \\
&\quad\times\frac{1}{\omega_1\lambda_{ip1}}\exp\left(-\frac{y}{\omega_1\lambda_{ip1}}\right)dxdy \\
&= \frac{1}{\lambda_{2E}}\frac{1}{\omega_1\lambda_{ip1}}\int_0^\infty\int_0^\infty\exp\left(-\left(\frac{\phi_E\left(\alpha_1\phi y+1\right)}{\phi\lambda_{2R}}+\frac{1}{\lambda_{2E}}\right)x\right) \\
&\quad\times\exp\left(-\frac{y}{\omega_1\lambda_{ip1}}\right)dxdy \\
&= \frac{1}{\omega_1\lambda_{ip1}}\int_0^\infty\frac{\phi\lambda_{2R}}{\phi_E\alpha_1\phi\lambda_{2E}y+\phi_E\lambda_{2E}+\phi\lambda_{2R}} \\
&\quad\times\exp\left(-\frac{y}{\omega_1\lambda_{ip1}}\right)dy. \qquad \text{(D.1)}
\end{aligned}$$

Based on [45, Eq. (3.352.4)] and applying some polynomial expansion manipulations, W_1 is written by

$$W_1 = -\frac{\lambda_{2R}}{\alpha_1\phi_E\lambda_{2E}\omega_1\lambda_{ip1}}\exp(\Phi_2)\,\mathrm{Ei}(-\Phi_2), \qquad \text{(D.2)}$$

where $\Phi_2 = \frac{\phi_E\lambda_{2E}+\phi\lambda_{2R}}{\alpha_1\phi\phi_E\lambda_{2E}\omega_1\lambda_{ip1}}$.

Next, W_2 can be calculated as

$$\begin{aligned}
W_2 &= \Pr\left[|h_{RS}|^2 > \frac{\phi_E|h_{RE}|^2\left(\beta_1\phi|\widetilde{h}_{D1S}|^2+1\right)}{\phi}\right] \\
&= \int_0^\infty\int_0^\infty\left(1-F_{|h_{RS}|^2}\left(\frac{\phi_E x\left(\beta_1\phi y+1\right)}{\phi}\right)\right)f_{|h_{RE}|^2}(x) \\
&\quad\times f_{|\widetilde{h}_{D1S}|^2}(y)\,dxdy \\
&= \int_0^\infty\int_0^\infty \exp\left(-\frac{\phi_E x\left(\beta_1\phi y+1\right)}{\phi\lambda_{RS}}\right)\frac{1}{\lambda_{RE}}\exp\left(-\frac{x}{\lambda_{RE}}\right) \\
&\quad\times\frac{1}{\omega_2\lambda_{ip2}}\exp\left(-\frac{y}{\omega_2\lambda_{ip2}}\right)dxdy \\
&= \frac{1}{\lambda_{RE}}\frac{1}{\omega_2\lambda_{ip2}}\int_0^\infty\int_0^\infty\exp\left(-\left(\frac{\phi_E\left(\beta_1\phi y+1\right)}{\phi\lambda_{RS}}+\frac{1}{\lambda_{RE}}\right)x\right) \\
&\quad\times\exp\left(-\frac{y}{\omega_2\lambda_{ip2}}\right)dxdy \\
&= \frac{1}{\omega_2\lambda_{ip2}}\int_0^\infty\frac{\phi\lambda_{RS}}{\phi_E\beta_1\phi\lambda_{RE}y+\phi_E\lambda_{RE}+\phi\lambda_{RS}} \\
&\quad\times\exp\left(-\frac{y}{\omega_2\lambda_{ip2}}\right)dy. \qquad \text{(D.3)}
\end{aligned}$$

Based on [45, Eq. (3.352.4)] and applying some polynomial expansion manipulations, W_2 is given by

$$W_2 = -\frac{\lambda_{RS}}{\beta_1\phi_E\lambda_{RE}\omega_2\lambda_{ip2}}\exp(\Phi_3)\,\mathrm{Ei}(-\Phi_3), \qquad \text{(D.4)}$$

where $\Phi_3 = \frac{\phi_E\lambda_{RE}+\phi\lambda_{RS}}{\beta_1\phi\phi_E\lambda_{RE}\omega_2\lambda_{ip2}}$.

Substituting (D.2) and (D.4) into (33), we can obtain (29). It is the end of the proof.

APPENDIX E
PROOF OF PROPOSITION 7

Similar (20), the SOP of D_1 with N antennas can be expressed as

$$SOP_{D1}^{(n^*)} = 1 - \underbrace{\Pr\left[\frac{1+\gamma_{D1,n^*-S}^{(p1)}}{1+\gamma_{D1,n^*-E}^{(p1)}} \geq \mu_1\right]}_{A_{1,n^*}} \times \underbrace{\Pr\left[\frac{1+\gamma_{y_1,n^*}^{(p2)}}{1+\gamma_{D1,n^*-E}^{(p2)}} < \mu_1\right]}_{A_{2,n^*}}. \qquad \text{(E.1)}$$

From (E.1), A_{1,n^*} can be calculated as (E.2), shown at the bottom of the next page.

Next, A_{2,n^*} can be calculated as (E.3), shown at the bottom of the next page.

Based on [45, Eq. (3.352.4)] and applying some polynomial expansion manipulations, A_{2,n^*} is written by

$$\begin{aligned}
A_{2,n^*} &= -\sum_{l=1}^{N}\sum_{t=1}^{N}\binom{N}{l}\binom{N}{t}(-1)^{l+t-2}\frac{t\lambda_{1S,n}}{l\mu_1\phi_E\beta_2\lambda_{1E,n}\lambda_{RS}} \\
&\quad\times\exp\left(\bar{\lambda}_n\theta_n-\frac{l\overline{\mu_1}}{\beta_1\phi\lambda_{1S,n}}\right)\mathrm{Ei}\left(-\bar{\lambda}_n\theta_n\right), \qquad \text{(E.4)}
\end{aligned}$$

where $\bar{\lambda}_n = \frac{l\overline{\mu_1}\beta_2}{\beta_1\lambda_{1S,n}}+\frac{1}{\lambda_{RS}}$, $\theta_n = \frac{l\mu_1\phi_E\lambda_{1E,n}+t\phi\lambda_{1S,n}}{l\mu_1\phi_E\phi\beta_2\lambda_{1E,n}}$.

Substituting (E.2) and (E.3) into (E.1), we can obtain (54). The proof is completed.

APPENDIX F
PROOF OF PROPOSITION 8

Similar (22), the SOP of $G_1 - D_2$ with M antennas can be expressed as

$$SOP_{D2}^{(G1,m^*)} = 1 - \underbrace{\Pr\left[\frac{1+\gamma_{R,1n^*m^*}^{(p1)}}{1+\gamma_{D2,m^*-E}^{(p1)}} \geq \mu_2\right]}_{B_{1,m^*}} \times \underbrace{\Pr\left[\frac{1+\gamma_{x_2,n^*}^{(p2)}}{1+\gamma_{D2,m^*-E}^{(p2)}} \geq \mu_2\right]}_{B_{2,m^*}}. \qquad \text{(F.1)}$$

From (F.1), B_{1,m^*} can be calculated as (F.2), shown at the middle of the next page.

Based on [45, Eq. (3.352.4)] and applying some polynomial expansion manipulations, B_{1,m^*} is written by

$$\begin{aligned}B_{1,m^*} &= -\sum_{m=1}^{M}\sum_{r=1}^{M}\sum_{l=1}^{N}\binom{M}{m}\binom{M}{r}\binom{N}{l}(-1)^{m+r+l-3}\\ &\times \frac{rl\lambda_{2R,m}}{m\mu_2\alpha_1\phi_E\omega_1\lambda_{ip1,n}\lambda_{2E,m}}\exp\left(\psi_{1,m}\delta_{1,m}-\frac{m\overline{\mu_2}}{\alpha_2\phi\lambda_{2R,m}}\right)\\ &\times \mathrm{Ei}\left(-\psi_{1,m}\delta_{1,m}\right),\end{aligned} \tag{F.3}$$

where $\psi_{1,m}=\frac{m\mu_2\phi_E\lambda_{2E,m}+r\phi\lambda_{2R,m}}{m\mu_2\alpha_1\phi\phi_E\lambda_{2E,m}}$, $\delta_{1,m}=\frac{m\overline{\mu_2}\alpha_1}{\alpha_2\lambda_{2R,m}}+\frac{l}{\omega_1\lambda_{ip1,n}}$.

Next, B_{2,m^*} can be calculated as (F.4), shown at the middle of the next page.

$$\begin{aligned}A_{1,n^*} &= \Pr\left[\gamma_{D1,n^*-S}^{(p1)}\geq\overline{\mu_1}+\mu_1\gamma_{D1,n^*-E}^{(p1)}\right]\\ &= \Pr\left[\left|h_{D1S,n^*}\right|^2\geq\frac{\overline{\mu_1}+\mu_1\alpha_1\phi_E\left|h_{D1E,n^*}\right|^2}{\alpha_1\phi}\right]\\ &= \int_0^\infty\left(1-F_{|h_{D1S,n^*}|^2}\left(\frac{\overline{\mu_1}+\mu_1\alpha_1\phi_E x}{\alpha_1\phi}\right)\right)f_{|h_{D1E,n^*}|^2}(x)\,dx\\ &= \sum_{n=1}^{N}\sum_{r=1}^{N}\binom{N}{n}\binom{N}{r}(-1)^{n+r-2}\frac{r}{\lambda_{1E,n}}\exp\left(-\frac{n\overline{\mu_1}}{\alpha_1\phi\lambda_{1S,n}}\right)\int_0^\infty\exp\left(-\left(\frac{n\mu_1\phi_E}{\phi\lambda_{1S,n}}+\frac{r}{\lambda_{1E,n}}\right)x\right)dx\\ &= \sum_{n=1}^{N}\sum_{r=1}^{N}\binom{N}{n}\binom{N}{r}(-1)^{n+r-2}\frac{r\phi\lambda_{1S,n}}{n\mu_1\phi_E\lambda_{1E,n}+r\phi\lambda_{1S,n}}\exp\left(-\frac{n\overline{\mu_1}}{\alpha_1\phi\lambda_{1S,n}}\right).\end{aligned} \tag{E.2}$$

$$\begin{aligned}A_{2,n^*} &= \Pr\left[\gamma_{y_1,n^*}^{(p2)}\geq\overline{\mu_1}+\mu_1\gamma_{D1,n^*-E}^{(p2)}\right]\\ &= \Pr\left[\left|h_{D1S,n^*}\right|^2\geq\frac{\left(\overline{\mu_1}+\mu_1\beta_1\phi_E\left|h_{D1E,n^*}\right|^2\right)\left(\beta_2\phi|h_{RS}|^2+1\right)}{\beta_1\phi}\right]\\ &= \int_0^\infty\int_0^\infty\left(1-F_{|h_{D1S,n^*}|^2}\left(\frac{(\overline{\mu_1}+\mu_1\beta_1\phi_E x)(\beta_2\phi y+1)}{\beta_1\phi}\right)\right)f_{|h_{D1E,n^*}|^2}(x)f_{|h_{RS}|^2}(y)\,dxdy\\ &= \sum_{l=1}^{N}\sum_{t=1}^{N}\binom{N}{l}\binom{N}{t}(-1)^{l+t-2}\frac{t}{\lambda_{1E,n}}\frac{1}{\lambda_{RS}}\exp\left(-\frac{l\overline{\mu_1}}{\beta_1\phi\lambda_{1S,n}}\right)\\ &\quad\times\int_0^\infty\int_0^\infty\exp\left(-\left(\frac{l\mu_1\phi_E\phi\beta_2 y+l\mu_1\phi_E}{\phi\lambda_{1S,n}}+\frac{t}{\lambda_{1E,n}}\right)x\right)\exp\left(-\left(\frac{l\overline{\mu_1}\beta_2}{\beta_1\lambda_{1S,n}}+\frac{1}{\lambda_{RS}}\right)y\right)dxdy\\ &= \sum_{l=1}^{N}\sum_{t=1}^{N}\binom{N}{l}\binom{N}{t}(-1)^{l+t-2}\frac{1}{\lambda_{RS}}\exp\left(-\frac{l\overline{\mu_1}}{\beta_1\phi\lambda_{1S,n}}\right)\\ &\quad\times\int_0^\infty\frac{t\phi\lambda_{1S,n}}{l\mu_1\phi_E\phi\beta_2\lambda_{1E,n}y+l\mu_1\phi_E\lambda_{1E,n}+t\phi\lambda_{1S,n}}\exp\left(-\left(\frac{l\overline{\mu_1}\beta_2}{\beta_1\lambda_{1S,n}}+\frac{1}{\lambda_{RS}}\right)y\right)dy.\end{aligned} \tag{E.3}$$

$$\begin{aligned}B_{1,m^*} &= \Pr\left[\gamma_{R,1n^*m^*}^{(p1)}\geq\overline{\mu_2}+\mu_2\gamma_{D2,m^*-E}^{(p1)}\right]\\ &= \Pr\left[\left|h_{D2R,m^*}\right|^2\geq\frac{\left(\overline{\mu_2}+\mu_2\alpha_2\phi_E\left|h_{D2E,m^*}\right|^2\right)\left(\alpha_1\phi\left|\widetilde{h}_{D1R,n^*}\right|^2+1\right)}{\alpha_2\phi}\right]\\ &= \int_0^\infty\int_0^\infty\left(1-F_{|h_{D2R,m^*}|^2}\left(\frac{(\overline{\mu_2}+\mu_2\alpha_2\phi_E x)(\alpha_1\phi y+1)}{\alpha_2\phi}\right)\right)f_{|h_{D2E,m^*}|^2}(x)f_{|\widetilde{h}_{D1R,n^*}|^2}(y)\,dxdy\\ &= \sum_{m=1}^{M}\sum_{r=1}^{M}\sum_{l=1}^{N}\binom{M}{m}\binom{M}{r}\binom{N}{l}(-1)^{m+r+l-3}\frac{r}{\lambda_{2E,m}}\frac{l}{\omega_1\lambda_{ip1,n}}\exp\left(-\frac{m\overline{\mu_2}}{\alpha_2\phi\lambda_{2R,m}}\right)\\ &\quad\times\int_0^\infty\int_0^\infty\exp\left(-\left(\frac{m\mu_2\alpha_1\phi\phi_E y+m\mu_2\phi_E}{\phi\lambda_{2R,m}}+\frac{r}{\lambda_{2E,m}}\right)x\right)\exp\left(-\left(\frac{m\overline{\mu_2}\alpha_1}{\alpha_2\lambda_{2R,m}}+\frac{l}{\omega_1\lambda_{ip1,n}}\right)y\right)dxdy\\ &= \sum_{m=1}^{M}\sum_{r=1}^{M}\sum_{l=1}^{N}\binom{M}{m}\binom{M}{r}\binom{N}{l}(-1)^{m+r+l-3}\frac{l}{\omega_1\lambda_{ip1,n}}\exp\left(-\frac{m\overline{\mu_2}}{\alpha_2\phi\lambda_{2R,m}}\right)\\ &\quad\times\int_0^\infty\frac{r\phi\lambda_{2R,k}}{m\mu_2\alpha_1\phi\phi_E\lambda_{2E,m}y+m\mu_2\phi_E\lambda_{2E,m}+r\phi\lambda_{2R,m}}\exp\left(-\left(\frac{m\overline{\mu_2}\alpha_1}{\alpha_2\lambda_{2R,m}}+\frac{l}{\omega_1\lambda_{ip1,n}}\right)y\right)dy.\end{aligned} \tag{F.2}$$

Based on [45, Eq. (3.352.4)] and applying some polynomial expansion manipulations, B_{2,m^*} is written by

$$B_{2,m^*} = -\sum_{t=1}^{N}\binom{N}{t}(-1)^{t-1}\frac{t\lambda_{RS}}{\mu_2\beta_1\phi_E\omega_2\lambda_{ip2,n}\lambda_{RE}} \times \exp\left(\psi_2\delta_{2,m} - \frac{\overline{\mu_2}}{\beta_2\phi\lambda_{RS}}\right)\mathrm{Ei}\left(-\psi_2\delta_{2,m}\right), \quad \text{(F.5)}$$

where $\delta_{2,m} = \frac{\overline{\mu_2}\beta_1}{\beta_2\lambda_{RS}} + \frac{t}{\omega_2\lambda_{ip2,n}}$.

Substituting (F.3) and (F.5) into (F.1), we can obtain (55). The proof is completed.

APPENDIX G
PROOF OF PROPOSITION 9

Similar (31), the SPSC of D_1 with N antennas can be expressed as

$$SPSC_{D1}^{(n^*)} = \underbrace{\Pr\left(\gamma_{D1,n^*-S}^{(p1)} > \gamma_{D1,n^*-E}^{(p1)}\right)}_{Q_{1,n^*}} \times \underbrace{\Pr\left(\gamma_{y_1,n^*}^{(p2)} > \gamma_{D1,n^*-E}^{(p2)}\right)}_{Q_{2,n^*}}. \quad \text{(G.1)}$$

From (G.1), Q_{1,n^*} can be calculated as

$$\begin{aligned} Q_{1,n^*} &= \Pr\left[\left|h_{D1S,n^*}\right|^2 \geq \frac{\phi_E\left|h_{D1E,n^*}\right|^2}{\phi}\right] \\ &= \int_0^\infty \left(1 - F_{|h_{D1S,n^*}|^2}\left(\frac{\phi_E x}{\phi}\right)\right) f_{|h_{D1E,n^*}|^2}(x)\,dx \\ &= \sum_{n=1}^{N}\sum_{r=1}^{N}\binom{N}{n}\binom{N}{r}(-1)^{n+r-2}\frac{r}{\lambda_{1E,n}} \\ &\quad \times \int_0^\infty \exp\left(-\left(\frac{n\phi_E}{\phi\lambda_{1S,n}} + \frac{r}{\lambda_{1E,n}}\right)x\right)dx \\ &= \sum_{n=1}^{N}\sum_{r=1}^{N}\binom{N}{n}\binom{N}{r}(-1)^{n+r-2}\frac{r\phi\lambda_{1S,n}}{n\phi_E\lambda_{1E,n} + r\phi\lambda_{1S,n}}. \end{aligned} \quad \text{(G.2)}$$

Next, Q_{2,n^*} can be calculated as (G.3), shown at the bottom of the next page.

Based on [45, Eq. (3.352.4)] and applying some polynomial expansion manipulations, Q_{2,n^*} is written by

$$Q_{2,n^*} = -\sum_{l=1}^{N}\sum_{t=1}^{N}\binom{N}{l}\binom{N}{t}(-1)^{l+t-2} \times \frac{t\lambda_{1S,n}}{l\beta_2\phi_E\lambda_{1E,n}\lambda_{RS}}\exp\left(\Phi_{1,n}\right)\mathrm{Ei}\left(-\Phi_{1,n}\right), \quad \text{(G.4)}$$

where $\Phi_{1,n} = \frac{l\phi_E\lambda_{1E,n} + t\phi\lambda_{1S,n}}{l\beta_2\phi_E\phi\lambda_{1E,n}\lambda_{RS}}$.

Substituting (G.2) and (G.4) into (G.1), we can obtain (56). The proof is completed.

APPENDIX H
PROOF OF PROPOSITION 10

Similar (33), the SPSC of $G_1 - D_1$ with M antennas can be expressed as

$$SPSC_{D2}^{(G1,m^*)} = \underbrace{\Pr\left[\gamma_{R,1n^*m^*}^{(p1)} > \gamma_{D2,m^*-E}^{(p1)}\right]}_{W_{1,m^*}} \times \underbrace{\Pr\left[\gamma_{x_2,n^*}^{(p2)} > \gamma_{D2,m^*-E}^{(p2)}\right]}_{W_{2,m^*}}. \quad \text{(H.1)}$$

From (H.1), W_{1,m^*} can be calculated as (H.2), shown at the bottom of the next page.

$$\begin{aligned} B_{2,m^*} &= \Pr\left[\gamma_{x_2,n^*}^{(p2)} \geq \overline{\mu_2} + \mu_2\gamma_{D2,m^*-E}^{(p2)}\right] \\ &= \Pr\left[|h_{RS}|^2 \geq \frac{\left(\overline{\mu_2} + \mu_2\beta_2\phi_E|h_{RE}|^2\right)\left(\beta_1\phi\left|\widetilde{h}_{D1S,n^*}\right|^2 + 1\right)}{\beta_2\phi}\right] \\ &= \int_0^\infty\int_0^\infty \left(1 - F_{|h_{RS}|^2}\left(\frac{\left(\overline{\mu_2} + \mu_2\beta_2\phi_E x\right)\left(\beta_1\phi y + 1\right)}{\beta_2\phi}\right)\right) f_{|h_{RE}|^2}(x) f_{\left|\widetilde{h}_{D1S,n^*}\right|^2}(y)\,dxdy \\ &= \sum_{t=1}^{N}\binom{N}{t}(-1)^{t-1}\frac{1}{\lambda_{RE}}\frac{t}{\omega_2\lambda_{ip2,n}}\exp\left(-\frac{\overline{\mu_2}}{\beta_2\phi\lambda_{RS}}\right) \\ &\quad \times \int_0^\infty\int_0^\infty \exp\left(-\left(\frac{\mu_2\beta_1\phi_E\phi y + \mu_2\phi_E}{\phi\lambda_{RS}} + \frac{1}{\lambda_{RE}}\right)x\right)\exp\left(-\left(\frac{\overline{\mu_2}\beta_1}{\beta_2\lambda_{RS}} + \frac{t}{\omega_2\lambda_{ip2,n}}\right)y\right)dxdy \\ &= \sum_{t=1}^{N}\binom{N}{t}(-1)^{t-1}\frac{t}{\omega_2\lambda_{ip2,n}}\exp\left(-\frac{\overline{\mu_2}}{\beta_2\phi\lambda_{RS}}\right) \\ &\quad \times \int_0^\infty \frac{\phi\lambda_{RS}}{\mu_2\beta_1\phi_E\phi\lambda_{RE}y + \mu_2\phi_E\lambda_{RE} + \phi\lambda_{RS}}\exp\left(-\left(\frac{\overline{\mu_2}\beta_1}{\beta_2\lambda_{RS}} + \frac{t}{\omega_2\lambda_{ip2,n}}\right)y\right)dy. \end{aligned} \quad \text{(F.4)}$$

Based on [45, Eq. (3.352.4)] and applying some polynomial expansion manipulations, W_{1,m^*} is written by

$$W_{1,m^*} = -\sum_{m=1}^{M}\sum_{r=1}^{M}\sum_{l=1}^{N}\binom{M}{m}\binom{M}{r}\binom{N}{l}(-1)^{m+r+l-3} \times \frac{rl\lambda_{2R,m}}{m\alpha_1\phi_E\lambda_{2E,m}\omega_1\lambda_{ip1,n}}\exp\left(\Phi_{2,m}\right)\mathrm{Ei}\left(-\Phi_{2,m}\right), \tag{H.3}$$

where $\Phi_{2,m} = \frac{lm\phi_E\lambda_{2E,m}+lr\phi\lambda_{2R,m}}{m\alpha_1\phi_E\lambda_{2E,m}\omega_1\lambda_{ip1,n}}$.

From (H.1), W_{2,m^*} can be calculated as (H.4), shown at the bottom of the page.

Based on [45, Eq. (3.352.4)] and applying some polynomial expansion manipulations, W_{2,m^*} is written by

$$W_{2,m^*} = -\sum_{t=1}^{N}\binom{N}{t}(-1)^{t-1}\frac{t\lambda_{RS}}{\beta_1\phi_E\lambda_{RE}\omega_2\lambda_{ip2,n}} \times \exp\left(\Phi_{3,m}\right)\mathrm{Ei}\left(-\Phi_{3,m}\right), \tag{H.5}$$

where $\Phi_{3,m} = \frac{t\phi_E\lambda_{RE}+t\phi\lambda_{RS}}{\beta_1\phi_E\lambda_{RE}\omega_2\lambda_{ip2,n}}$.

Substituting (H.3) and (H.5) into (H.1), we can obtain (57). The proof is completed.

$$\begin{aligned}
Q_{2,n^*} &= \Pr\left[\left|h_{D1S,n^*}\right|^2 \geq \frac{\phi_E\left|h_{D1E,n^*}\right|^2\left(\beta_2\phi|h_{RS}|^2+1\right)}{\phi}\right] \\
&= \int_0^\infty\int_0^\infty\left(1-F_{|h_{D1S,n^*}|^2}\left(\frac{\phi_E x\left(\beta_2\phi y+1\right)}{\phi}\right)\right)f_{|h_{D1E,n^*}|^2}(x)f_{|h_{RS}|^2}(y)\,dxdy \\
&= \sum_{l=1}^{N}\sum_{t=1}^{N}\binom{N}{l}\binom{N}{t}(-1)^{l+t-2}\frac{t}{\lambda_{1E,n}}\frac{1}{\lambda_{RS}}\int_0^\infty\int_0^\infty\exp\left(-\left(\frac{l\phi_E\phi\beta_2 y+l\phi_E}{\phi\lambda_{1S,n}}+\frac{t}{\lambda_{1E,n}}\right)x\right)\exp\left(-\frac{y}{\lambda_{RS}}\right)dxdy \\
&= \sum_{l=1}^{N}\sum_{t=1}^{N}\binom{N}{l}\binom{N}{t}(-1)^{l+t-2}\frac{1}{\lambda_{RS}}\int_0^\infty\frac{t\phi\lambda_{1S,n}}{l\phi_E\phi\beta_2\lambda_{1E,n}y+l\phi_E\lambda_{1E,n}+t\phi\lambda_{1S,n}}\exp\left(-\frac{y}{\lambda_{RS}}\right)dy.
\end{aligned} \tag{G.3}$$

$$\begin{aligned}
W_{1,m^*} &= \Pr\left[\left|h_{D2R,m^*}\right|^2 > \frac{\phi_E\left|h_{D2E,m^*}\right|^2\left(\alpha_1\phi\left|\widetilde{h}_{D1R,n^*}\right|^2+1\right)}{\phi}\right] \\
&= \int_0^\infty\int_0^\infty\left(1-F_{|h_{D2R,m^*}|^2}\left(\frac{\phi_E x\left(\alpha_1\phi y+1\right)}{\phi}\right)\right)f_{|h_{D2E,m^*}|^2}(x)f_{|\widetilde{h}_{D1R,n^*}|^2}(y)\,dxdy \\
&= \sum_{m=1}^{M}\sum_{r=1}^{M}\sum_{l=1}^{N}\binom{M}{m}\binom{M}{r}\binom{N}{l}(-1)^{m+r+l-3}\frac{r}{\lambda_{2E,m}}\frac{l}{\omega_1\lambda_{ip1,n}} \\
&\quad\times\int_0^\infty\int_0^\infty\exp\left(-\left(\frac{m\alpha_1\phi\phi_E y+m\phi_E}{\phi\lambda_{2R,m}}+\frac{r}{\lambda_{2E,m}}\right)x\right)\exp\left(-\frac{ly}{\omega_1\lambda_{ip1,n}}\right)dxdy \\
&= \sum_{m=1}^{M}\sum_{r=1}^{M}\sum_{l=1}^{N}\binom{M}{m}\binom{M}{r}\binom{N}{l}(-1)^{m+r+l-3}\frac{l}{\omega_1\lambda_{ip1,n}}\int_0^\infty\frac{r\phi\lambda_{2R,m}}{m\alpha_1\phi\phi_E\lambda_{2E,m}y+m\phi_E\lambda_{2E,m}+r\phi\lambda_{2R,m}}\exp\left(-\frac{ly}{\omega_1\lambda_{ip1,n}}\right)dy.
\end{aligned} \tag{H.2}$$

$$\begin{aligned}
W_{2,m^*} &= \Pr\left[|h_{RS}|^2 \geq \frac{\phi_E|h_{RE}|^2\left(\beta_1\phi\left|\widetilde{h}_{D1S,n^*}\right|^2+1\right)}{\phi}\right] \\
&= \int_0^\infty\int_0^\infty\left(1-F_{|h_{RS}|^2}\left(\frac{\phi_E x\left(\beta_1\phi y+1\right)}{\phi}\right)\right)f_{|h_{RE}|^2}(x)f_{|\widetilde{h}_{D1S,n^*}|^2}(y)\,dxdy \\
&= \sum_{t=1}^{N}\binom{N}{t}(-1)^{t-1}\frac{1}{\lambda_{RE}}\frac{t}{\omega_2\lambda_{ip2,n}}\int_0^\infty\int_0^\infty\exp\left(-\left(\frac{\beta_1\phi_E\phi y+\phi_E}{\phi\lambda_{RS}}+\frac{1}{\lambda_{RE}}\right)x\right)\exp\left(-\frac{ty}{\omega_2\lambda_{ip2,n}}\right)dxdy \\
&= \sum_{t=1}^{N}\binom{N}{t}(-1)^{t-1}\frac{t}{\omega_2\lambda_{ip2,n}}\int_0^\infty\frac{\phi\lambda_{RS}}{\beta_1\phi_E\phi\lambda_{RE}y+\phi_E\lambda_{RE}+\phi\lambda_{RS}}\exp\left(-\frac{ty}{\omega_2\lambda_{ip2,n}}\right)dy.
\end{aligned} \tag{H.4}$$

REFERENCES

[1] S. M. R. Islam, N. Avazov, O. A. Dobre, and K.-S. Kwak, "Power-domain non-orthogonal multiple access (NOMA) in 5G systems: Potentials and challenges," *IEEE Commun. Surveys Tuts.*, vol. 19, no. 2, pp. 721–742, 2nd Quart., 2017.

[2] F. Zhou, Y. Wu, Y.-C. Liang, Z. Li, Y. Wang, and K.-K. Wong, "State of the art, taxonomy, and open issues on cognitive radio networks with NOMA," *IEEE Wireless Commun.*, vol. 25, no. 2, pp. 100–108, Apr. 2018.

[3] S. M. R. Islam, M. Zeng, and O. A. Dobre, "NOMA in 5G systems: Exciting possibilities for enhancing spectral efficiency," *IEEE 5G Tech Focus*, vol. 1, no. 2, pp. 1–6, Jun. 2017.

[4] Y. Liu, Z. Qin, M. Elkashlan, Y. Gao, and L. Hanzo, "Enhancing the physical layer security of non-orthogonal multiple access in large-scale networks," *IEEE Trans. Wireless Commun.*, vol. 16, no. 3, pp. 1656–1672, Mar. 2017.

[5] H. Lei, R. Gao, K.-H. Park, I. S. Ansari, K. J. Kim, and M.-S. Alouini, "On secure downlink NOMA systems with outage constraint," *IEEE Trans. Commun.*, vol. 68, no. 12, pp. 7824–7836, Dec. 2020.

[6] S. Chen, B. Ren, Q. Gao, S. Kang, S. Sun, and K. Niu, "Pattern division multiple access—A novel nonorthogonal multiple access for fifth-generation radio networks," *IEEE Trans. Veh. Technol.*, vol. 66, no. 4, pp. 3185–3196, Apr. 2017.

[7] B. Zheng, M. Wen, F. Chen, J. Tang, and F. Ji, "Secure NOMA based full-duplex two-way relay networks with artificial noise against eavesdropping," in *Proc. IEEE Int. Conf. Commun. (ICC)*, Kansas City, MO, USA, May 2018, pp. 1–6.

[8] Z. Ding, Y. Liu, J. Choi, Q. Sun, M. Elkashlan, I. Chih-Lin, and H. V. Poor, "Application of non-orthogonal multiple access in LTE and 5G networks," *IEEE Commun. Mag.*, vol. 55, no. 2, pp. 185–191, Feb. 2017.

[9] Z. Ding, M. Peng, and H. V. Poor, "Cooperative non-orthogonal multiple access in 5G systems," *IEEE Commun. Lett.*, vol. 19, no. 8, pp. 1462–1465, Aug. 2015.

[10] Y. Ji, W. Duan, M. Wen, P. Padidar, J. Li, N. Cheng, and P.-H. Ho, "Spectral efficiency enhanced cooperative device-to-device systems with NOMA," *IEEE Trans. Intell. Transp. Syst.*, early access, Jul. 17, 2020, doi: 10.1109/TITS.2020.3006857.

[11] D.-T. Do, T.-L. Nguyen, K. M. Rabie, X. Li, and B. M. Lee, "Throughput analysis of multipair two-way replaying networks with NOMA and imperfect CSI," *IEEE Access*, vol. 8, pp. 128942–128953, 2020.

[12] X. Liang, Y. Wu, D. W. K. Ng, Y. Zuo, S. Jin, and H. Zhu, "Outage performance for cooperative NOMA transmission with an AF relay," *IEEE Commun. Lett.*, vol. 21, no. 11, pp. 2428–2431, Nov. 2017.

[13] H.-P. Dang, M.-S. Van Nguyen, D.-T. Do, H.-L. Pham, B. Selim, and G. Kaddoum, "Joint relay selection, full-duplex and device-to-device transmission in wireless powered NOMA networks," *IEEE Access*, vol. 8, pp. 82442–82460, 2020.

[14] D.-T. Do, A.-T. Le, C.-B. Le, and B. M. Lee, "On exact outage and throughput performance of cognitive radio based non-orthogonal multiple access networks with and without D2D link," *Sensors*, vol. 19, no. 15, p. 3314, Jul. 2019.

[15] D.-T. Do, A.-T. Le, and B. M. Lee, "NOMA in cooperative underlay cognitive radio networks under imperfect SIC," *IEEE Access*, vol. 8, pp. 86180–86195, 2020.

[16] D.-T. Do, M.-S. Van Nguyen, T.-A. Hoang, and B. M. Lee, "Exploiting joint base station equipped multiple antenna and full-duplex D2D users in power domain division based multiple access networks," *Sensors*, vol. 19, no. 11, p. 2475, May 2019.

[17] A. Yener and S. Ulukus, "Wireless physical-layer security: Lessons learned from information theory," *Proc. IEEE*, vol. 103, no. 10, pp. 1814–1825, Oct. 2015.

[18] A. D. Wyner, "The wire-tap channel," *Bell Syst. Tech. J.*, vol. 54, no. 8, pp. 1355–1387, Oct. 1975.

[19] T. Bilski, "New threats and innovative protection methods in wireless transmission systems," *J. Telecommun. Inf. Technol.*, vol. 3, pp. 26–33, Mar. 2014.

[20] Y.-S. Shiu, S. Chang, H.-C. Wu, S. Huang, and H.-H. Chen, "Physical layer security in wireless networks: A tutorial," *IEEE Wireless Commun.*, vol. 18, no. 2, pp. 66–74, Apr. 2011.

[21] Y. Jiang, Y. Zou, J. Ouyang, and J. Zhu, "Secrecy energy efficiency optimization for artificial noise aided physical-layer security in OFDM-based cognitive radio networks," *IEEE Trans. Veh. Technol.*, vol. 67, no. 12, pp. 11858–11872, Dec. 2018.

[22] L. Ni, X. Da, H. Hu, Y. Huang, R. Xu, and M. Zhang, "Outage constrained robust transmit design for secure cognitive radio with practical energy harvesting," *IEEE Access*, vol. 6, pp. 71444–71454, 2018.

[23] H. Lei, Z. Dai, K.-H. Park, W. Lei, G. Pan, and M.-S. Alouini, "Secrecy outage analysis of mixed RF-FSO downlink SWIPT systems," *IEEE Trans. Commun.*, vol. 66, no. 12, pp. 6384–6395, Dec. 2018.

[24] X. Chen, D. W. K. Ng, W. H. Gerstacker, and H.-H. Chen, "A survey on multiple-antenna techniques for physical layer security," *IEEE Commun. Surveys Tuts.*, vol. 19, no. 2, pp. 1027–1053, 2nd Quart., 2017.

[25] O. S. Badarneh, P. C. Sofotasios, S. Muhaidat, S. L. Cotton, K. M. Rabie, and N. Aldhahir, "Achievable physical-layer security over composite fading channels," *IEEE Access*, vol. 8, pp. 195772–195787, 2020.

[26] W. M. R. Shakir, "Physical layer security performance analysis of hybrid FSO/RF communication system," *IEEE Access*, vol. 9, pp. 18948–18961, 2021.

[27] N. A. Sarker, A. S. M. Badrudduza, S. M. R. Islam, S. H. Islam, I. S. Ansari, M. K. Kundu, M. F. Samad, M. B. Hossain, and H. Yu, "Secrecy performance analysis of mixed hyper-gamma and gamma-gamma cooperative relaying system," *IEEE Access*, vol. 8, pp. 131273–131285, 2020.

[28] H. Wang, L. Xu, W. Lin, P. Xiao, and R. Wen, "Physical layer security performance of wireless mobile sensor networks in smart city," *IEEE Access*, vol. 7, pp. 15436–15443, 2019.

[29] X. Yue, Y. Liu, Y. Yao, X. Li, R. Liu, and A. Nallanathan, "Secure communications in a unified non-orthogonal multiple access framework," *IEEE Trans. Wireless Commun.*, vol. 19, no. 3, pp. 2163–2178, Mar. 2020.

[30] H. Wei, D. Wang, X. Hou, Y. Zhu, and J. Zhu, "Secrecy analysis for massive MIMO systems with internal eavesdroppers," in *Proc. IEEE 82nd Veh. Technol. Conf. (VTC-Fall)*, Boston, MA, USA, Sep. 2015, pp. 1–5.

[31] Y. Li, M. Jiang, Q. Zhang, Q. Li, and J. Qin, "Secure beamforming in downlink MISO nonorthogonal multiple access systems," *IEEE Trans. Veh. Technol.*, vol. 66, no. 8, pp. 7563–7567, Aug. 2017.

[32] B. M. ElHalawany and K. Wu, "Physical-layer security of NOMA systems under untrusted users," in *Proc. IEEE Global Commun. Conf. (GLOBECOM)*, Abu Dhabi, United Arab Emirates, Dec. 2018, pp. 1–6.

[33] K. Cao, B. Wang, H. Ding, T. Li, and F. Gong, "Optimal relay selection for secure NOMA systems under untrusted users," *IEEE Trans. Veh. Technol.*, vol. 69, no. 2, pp. 1942–1955, Feb. 2020.

[34] L. Lv, H. Jiang, Z. Ding, L. Yang, and J. Chen, "Secrecy-enhancing design for cooperative downlink and uplink NOMA with an untrusted relay," *IEEE Trans. Commun.*, vol. 68, no. 3, pp. 1698–1715, Mar. 2020.

[35] K. Jiang, W. Zhou, and L. Sun, "Jamming-aided secrecy performance in secure uplink NOMA system," *IEEE Access*, vol. 8, pp. 15072–15084, 2020.

[36] Z. Xiang, W. Yang, Y. Cai, Z. Ding, Y. Song, and Y. Zou, "NOMA-assisted secure short-packet communications in IoT," *IEEE Wireless Commun.*, vol. 27, no. 4, pp. 8–15, Aug. 2020.

[37] M. Zeng, N.-P. Nguyen, O. A. Dobre, and H. V. Poor, "Securing downlink massive MIMO-NOMA networks with artificial noise," *IEEE J. Sel. Topics Signal Process.*, vol. 13, no. 3, pp. 685–699, Jun. 2019.

[38] Y. Zhang, H. Cao, M. Zhou, and L. Yang, "Spectral efficiency maximization for uplink cell-free massive MIMO-NOMA networks," in *Proc. IEEE Int. Conf. Commun. Workshops (ICC Workshops)*, Shanghai, China, May 2019, pp. 1–6.

[39] H. Lei, Z. Yang, K.-H. Park, I. S. Ansari, Y. Guo, G. Pan, and M.-S. Alouini, "Secrecy outage analysis for cooperative NOMA systems with relay selection schemes," *IEEE Trans. Commun.*, vol. 67, no. 9, pp. 6282–6298, Sep. 2019.

[40] M. S. Ali, H. Tabassum, and E. Hossain, "Dynamic user clustering and power allocation for uplink and downlink non-orthogonal multiple access (NOMA) systems," *IEEE Access*, vol. 4, pp. 6325–6343, 2016.

[41] Z. Yang, Z. Ding, P. Fan, and N. Al-Dhahir, "A general power allocation scheme to guarantee quality of service in downlink and uplink NOMA systems," *IEEE Trans. Wireless Commun.*, vol. 15, no. 11, pp. 7244–7257, Nov. 2016.

[42] M. F. Kader and S. Y. Shin, "Coordinated direct and relay transmission using uplink NOMA," *IEEE Wireless Commun. Lett.*, vol. 7, no. 3, pp. 400–403, Jun. 2018.

[43] J. Chen, L. Yang, and M.-S. Alouini, "Physical layer security for cooperative NOMA systems," *IEEE Trans. Veh. Technol.*, vol. 67, no. 5, pp. 4645–4649, May 2018.

[44] N.-P. Nguyen, T. Q. Duong, H. Q. Ngo, Z. Hadzi-Velkov, and L. Shu, "Secure 5G wireless communications: A joint relay selection and wireless power transfer approach," *IEEE Access*, vol. 4, pp. 3349–3359, 2016.

[45] I. S. Gradshteyn and I. M. Ryzhik, *Table of Integrals, Series and Products*, 6th ed. New York, NY, USA: Academic, 2000.
[46] K. Cao, B. Wang, H. Ding, L. Lv, J. Tian, and F. Gong, "On the security enhancement of uplink NOMA systems with jammer selection," *IEEE Trans. Commun.*, vol. 68, no. 9, pp. 5747–5763, Sep. 2020.
[47] L. Lv, Q. Ye, Z. Ding, Z. Li, N. Al-Dhahir, and J. Chen, "Multi-antenna two-way relay based cooperative NOMA," *IEEE Trans. Wireless Commun.*, vol. 19, no. 10, pp. 6486–6503, Oct. 2020.
[48] L. Fan, N. Yang, T. Q. Duong, M. Elkashlan, and G. K. Karagiannidis, "Exploiting direct links for physical layer security in multiuser multirelay networks," *IEEE Trans. Wireless Commun.*, vol. 15, no. 6, pp. 3856–3867, Jun. 2016.
[49] B. Xia, J. Wang, K. Xiao, Y. Gao, Y. Yao, and S. Ma, "Outage performance analysis for the advanced Sic receiver in wireless NOMA systems," *IEEE Trans. Veh. Technol.*, vol. 67, no. 7, pp. 6711–6715, Jul. 2018.
[50] L. Lv, Q. Ni, Z. Ding, and J. Chen, "Application of non-orthogonal multiple access in cooperative spectrum-sharing networks over Nakagami-*m* fading channels," *IEEE Trans. Veh. Technol.*, vol. 66, no. 6, pp. 5506–5511, Jun. 2017.
[51] Y. Xiao, L. Hao, Z. Ma, Z. Ding, Z. Zhang, and P. Fan, "Forwarding strategy selection in dual-hop NOMA relaying systems," *IEEE Commun. Lett.*, vol. 22, no. 8, pp. 1644–1647, Aug. 2018.
[52] G. Im and J. H. Lee, "Outage probability for cooperative NOMA systems with imperfect SIC in cognitive radio networks," *IEEE Commun. Lett.*, vol. 23, no. 4, pp. 692–695, Apr. 2019.

MINH-SANG VAN NGUYEN was born in Bentre, Vietnam. He is currently pursuing the master's degree in wireless communications. He worked with the Industrial University of Ho Chi Minh City, Vietnam. His research interests include electronic design, signal processing in wireless communications networks, non-orthogonal multiple access, and physical layer security.

DINH-THUAN DO (Senior Member, IEEE) received the B.S., M.Eng., and Ph.D. degrees from Vietnam National University (VNU-HCM) in 2003, 2007, and 2013, respectively, all in Communications Engineering. From 2003 to 2009, he was a Senior Engineer with VinaPhone Mobile Network. From 2009 to 2010, he was a Visiting Ph.D. Student with the Communications Engineering Institute, National Tsing Hua University, Taiwan. He published more than 85 SCI/SCIE journal articles. His research interests include signal processing in wireless communications networks, reconfigurable intelligent surfaces, non-orthogonal multiple access, full-duplex transmission, and energy harvesting. In 2015, he was recipient of the Golden Globe Award from the Vietnam Ministry of Science and Technology (Top ten excellent young scientists nationwide). He is currently serving as an Associate Editor for *EURASIP Journal on Wireless Communications and Networking*, *Computer Communications* (Elsevier), and *KSII Transactions on Internet and Information Systems*.

FATEMEH AFGHAH (Senior Member, IEEE) was an Assistant Professor with the Electrical and Computer Engineering Department, North Carolina Agricultural and Technical State University, Greensboro, NC, USA, from 2013 to 2015. She is currently an Associate Professor with the School of Informatics, Computing and Cyber Systems, Northern Arizona University (NAU), Flagstaff, AZ, USA, where she is the Director of the Wireless Networking and Information Processing (WiNIP) Laboratory. Her research interests include wireless communication networks, decision making in multi-agent systems, radio spectrum management, hardware-based security, and artificial intelligence in healthcare. She was a recipient of several awards, including the NSF CRII Award, in 2017, the Air Force Office of Scientific Research Young Investigator Award, in 2019, and the National Science Foundation (NSF) CAREER Award, in 2020.

S. M. RIAZUL ISLAM (Member, IEEE) was affiliated with the Memorial University, Canada as a Postdoctoral Fellow. Before that, he was with the University of Dhaka, Bangladesh, as an Assistant Professor and a Lecturer with the Department of Electrical and Electronic Engineering. He worked as a Chief Engineer with Samsung R&D Institute Bangladesh, Department of Solution Laboratory for advanced research. He is currently an Assistant Professor with the Department of Computer Science and Engineering, Sejong University, South Korea. Prior to joining Sejong, he worked as a Postdoctoral Fellow with the Wireless Communications Research Center, Inha University, South Korea. His research interests include wireless communications, the Internet of Things, and applied artificial intelligence.

ANH-TU LE was born in Lam Dong, Vietnam, in 1997. He is currently pursuing the master's degree in communications and information system, with a focus on wireless communications. He is a Research Assistant with the WICOM Laboratory led by Dr. Thuan. His research interests include wireless channel modeling, NOMA, cognitive radio, and MIMO.